



NTNU – Trondheim
Norwegian University of
Science and Technology

Development of new mechanical design of model turbines

Kristoffer Rundhaug

Mechanical Engineering

Submission date: July 2014

Supervisor: Ole Gunnar Dahlhaug, EPT

Co-supervisor: Torbjørn K. Nielsen, EPT

Norwegian University of Science and Technology
Department of Energy and Process Engineering



Norwegian University
of Science and Technology

Department of Energy
and Process Engineering

EPT-M-2014-100

MASTER THESIS

for

Kristoffer Rundhaug

Spring 2014

Development of new mechanical design of model turbines *Utvikling av nye mekanisk design av modell turbiner*

Background

The production of model Francis turbines to be used in the Waterpower laboratory at NTNU is a lengthy and costly process. The arrival of rapid prototyping opens up for new mechanical design for Kaplan, Francis and Pelton turbines. The combination parts manufactured by traditional production and rapid prototyping can be a faster and less costly process. This will be tested on one of the model turbines in the Waterpower laboratory.

Objective

Develop new mechanical design of a model Francis runner

The following tasks are to be considered:

1. Literature survey
 - a. Hydraulic design of high head Francis turbine runner and guide vanes
 - b. Mechanical design of high head Francis turbine runner and guide vanes
2. Software knowledge
 - a. Get familiar with the CAD-tool; ProEngineer/ Creo
3. Production of new runner blades for a Francis model turbine
4. Model tests (this will be carried out if the new blades will be available before the end of the semester)
 - a. Performance of the model turbine with new blades
5. Evaluation of alternative mechanical designs for:
 - a. Francis turbine runner
 - b. Guide vanes
 - c. Stay vanes

-- " --

Within 14 days of receiving the written text on the master thesis, the candidate shall submit a research plan for his project to the department.

When the thesis is evaluated, emphasis is put on processing of the results, and that they are presented in tabular and/or graphic form in a clear manner, and that they are analyzed carefully.

The thesis should be formulated as a research report with summary both in English and Norwegian, conclusion, literature references, table of contents etc. During the preparation of the text, the candidate should make an effort to produce a well-structured and easily readable report. In order to ease the evaluation of the thesis, it is important that the cross-references are correct. In the making of the report, strong emphasis should be placed on both a thorough discussion of the results and an orderly presentation.

The candidate is requested to initiate and keep close contact with his/her academic supervisor(s) throughout the working period. The candidate must follow the rules and regulations of NTNU as well as passive directions given by the Department of Energy and Process Engineering.

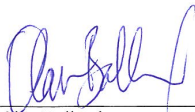
Risk assessment of the candidate's work shall be carried out according to the department's procedures. The risk assessment must be documented and included as part of the final report. Events related to the candidate's work adversely affecting the health, safety or security, must be documented and included as part of the final report. If the documentation on risk assessment represents a large number of pages, the full version is to be submitted electronically to the supervisor and an excerpt is included in the report.

Pursuant to "Regulations concerning the supplementary provisions to the technology study program/Master of Science" at NTNU §20, the Department reserves the permission to utilize all the results and data for teaching and research purposes as well as in future publications.

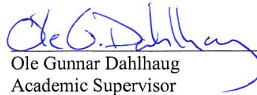
The final report is to be submitted digitally in DAIM. An executive summary of the thesis including title, student's name, supervisor's name, year, department name, and NTNU's logo and name, shall be submitted to the department as a separate pdf file. Based on an agreement with the supervisor, the final report and other material and documents may be given to the supervisor in digital format.

- Work to be done in the Waterpower laboratory
 Field work

Department of Energy and Process Engineering, 14. January 2014



Olav Bolland
Department Head



Ole Gunnar Dahlhaug
Academic Supervisor

Research Advisor/ co-supervisor:
Torbjørn K. Nielsen, Professor

torbjorn.nielsen@ntnu.no

Preface

This master thesis has been written at the Waterpower Laboratory, Department of Energy and Process Engineering at the Norwegian University of Science and Technology (NTNU) during the spring semester of 2014. The aim of this thesis was to come up with a new mechanical design of a Francis model runner.

I would like to thank my supervisor Ole Gunnar Dahlhaug for his guidance and support during this semester.

A special thanks to the PhD. candidates Bjørn Winther Solemslie and Peter Joachim Gogstad for great support and discussions. They have also been very helpful with knowledge of the CAD program Creo Parametric and the MATLAB design program Khoj.

In addition I would like to thank the rest of the staff at the Waterpower Laboratory, and especially Trygve Opland for helping me weld the test rig, and Bård Aslak Brandåstrø and Joar Grilstad for helping with parts needed for the testing.

I would also like to thank Anders Flaten at Protolab AS for taking time to meet and discuss designs and manufacturing methods.

And at last, I would like to thank all my fellow students at the Waterpower Laboratory for all good discussions and the great working environment.

Trondheim, July 22, 2014



Kristoffer Rundhaug

Abstract

The production of model Francis runner to be used in the Waterpower laboratory at NTNU is a lengthy and costly process. Due to the production cost there are years between each time a new Francis model is bought. The Tokke Francis model at Waterpower laboratory, was given from the industry after they had run model tests in the laboratory when designing the Tokke prototype.

In order to give the students at the Waterpower laboratory an opportunity to design their own turbines and test, the production cost must be significantly reduced. To be able to do that, new designs need to be developed and new production methods used.

The objective of this thesis is to carry out a new mechanical design of a Francis model runner and evaluate different mechanical designs of guide vanes and stay vanes. The new alternative designs were made with a combination of standard production methods and material, and new plastic materials from rapid prototyping such as selective laser sintering (SLS) and rapid CNC machining.

To carry out the new mechanical runner design, the MATLAB design software Khoj was used. From Khoj two sets of streamlines were generated, one set for the suction side and one for the pressure side. Then the streamlines were imported into the CAD program PTC Creo Parametric and a 3D-model of the design was made.

Two test pieces in a polyamide material were made using selective laser sintering. One of the test pieces was tested for pull-out strength using some self-tapping thread inserts, the results showed that the pull-out strength was more than good enough. The threaded insert could be used to attach the runner vanes to the hub and ring.

The main focus of this thesis has been the new mechanical design of a model runner and runner vanes. The model design was not produced and tested in the laboratory due to lack of time and money.

Sammendrag

Produksjonen av Francis modellturbiner for testing på Vannkraftlaboratoriet ved NTNU er omstendig og kostbar prosess. På grunn av de høye kostnadene er ofte flere år mellom hver gang en ny Francis modellturbin blir kjøpt. Tokke modellturbinen som nå brukes ved Vannkraftlaboratoriet var en gave fra industrien etter at den ble brukt til modelltesting da de designet Tokke prototype løpehjulet.

For å gi studenter ved Vannkraftlaboratoriet mulighet til å prøve seg på å lage egne turbindesign og test, må produksjonskostnadene reduseres kraftig. For å kutte kostnadene må nye design utvikles og nye produksjonsmetoder må tas i bruk.

Denne masteroppgaven har som mål å komme opp med et nytt mekanisk design av en Francis modellturbin, og evaluere forskjellige mekaniske design av ledeskovler og stagskovler. Disse nye alternative designene var produsert med en kombinasjon av standard materialer og produksjonsmetoder, og ved å ta i bruk nye plastmaterialer og rapid prototyping metoder som selective laser sintering (SLS) og rapid CNC maskinering.

For å utvikle det nye mekaniske løpehjul designet, ble MATLAB design programmet Khoj brukt. Fra Khoj ble to sett med strømningslinjer generert, et sett for trykksiden og et sett for sugesiden av skovlen. Strømningslinjene ble så importert inn i CAD programmet PTC Creo Parametric, hvor de ble brukt til å lage en 3D-modell av skovlen og det nye designet.

To test klosser laget av polyamid ble laget ved hjelp av SLS printing. En av klossene ble testet for hvor stor uttrykkskraft som skulle til for å dra ut en selvskruende gjengehylse. Resultatet viste at styrken var mer enn god nok til at hylsene kunne brukes til innfesting av skovlene mot hub og ring.

Hovedfokuset i denne masteroppgaven har vært det nye mekaniske løpehjul og skovl designet. Det ble uheldigvis ikke tid til å produsere det nye løpehjulet med ny hub og ring, og skovler i plast. Dette var på grunn av mangel på tid og penger.

Table of Contents

Preface	iii
Abstract	iv
Sammendrag	v
Table of Contents	ix
List of Tables	xi
List of Figures	xiv
Abbreviations	xv
1 Introduction	1
1.1 Objectives	1
1.2 Background	1
2 Theory	3
2.1 High head Francis turbine design	3
2.1.1 Main Dimensions	4
2.1.2 Energy Distributions	9
2.1.3 Simplified calculations on a high head Francis runner	10
2.2 Guide vanes	12
2.2.1 Hydraulic force acting on guide vanes	12
2.3 Stay ring and Stay vanes	13
2.4 CAD-Tool	13
2.5 Design software - Khoj	13
2.6 Selective Laser Sintering - SLS	14
2.7 Rapid CNC Machining	16
2.8 Materials used in prototype and model turbines	16

3	Mechanical turbine design	17
3.1	New mechanical design of model turbines	17
3.1.1	Francis model runner design	17
3.1.2	Guide vane design	22
3.1.3	Stay vane and stay ring design	25
4	Method	27
4.1	How to design a Francis runner to be used in the laboratory	27
4.1.1	Turbine design in MATLAB program Khoj	27
4.1.2	Drawing of a Francis runner vane in Creo Parametric	31
4.1.3	Drawing hub and ring in Creo Parametric	34
5	Experiment	37
5.1	Material tests	37
5.1.1	Test 1: Pull-out strength test	38
5.1.2	Test 2: Compression test	39
5.1.3	Test 3: Torque test	39
5.2	Results from material tests	40
6	Discussion	41
6.1	The new runner and runner vane designs	41
6.2	The new guide vane and stay vane designs	42
6.3	Manufacturing methods and materials	43
6.4	Production of runner blades and model test	44
6.5	FEM analysis of the new runner design	44
7	Conclusion	45
7.1	Conclusion	45
8	Further Work	47
8.1	Further Work	47
	Bibliography	49
A	Appendix A	i
A.1	Guide vane calculations	i
A.1.1	Hydraulic force on guide vane in closed position	ii
B	Appendix B	iii
B.1	Price offer from Protolab AS	iii
B.1.1	Price on	iii
C	Appendix C	ix
C.1	Material properties	ix
D	Appendix D	xiii
D.1	Drawings and documents from Tokke model turbine	xiii

E Appendix E	xix
E.1 Product information sheets for the fixing parts	xix

List of Tables

4.1 Input data from Tokk used in Khoj [4] 27

A.1 Data from Tokke model test used in calculations i

List of Figures

2.1	Axial view of high head Francis runner [12]	3
2.2	Velocity Triangles [10]	4
2.3	Velocity Triangles corrected [12]	6
2.4	Thoma cavitation coefficient [12]	7
2.5	The figure are showing $U \cdot C_u$ blade loading from inlet to outlet [12].	9
2.6	Principal sketch of high head Francis runner [3]	10
2.7	Model of runner for strength calculations [3].	10
2.8	Principal sketch of high head Francis runner [3]	11
2.9	Laser sintering and laser melting; contouring and recoating process [7, p.41]	14
3.1	3D-model of the Tokke model runner at NTNU	17
3.2	3D-model of the Runner and runner vanes Design 1	18
3.3	3D-model of the Runner and runner vanes Design 2	19
3.4	3D-model of the Runner and runner vanes Design 3	20
3.5	3D-model of the Runner and runner vanes Design 4	21
3.6	This figure show how the runner vanes in Design 4 will be attached to the hub and ring.	22
3.7	This figure shows the $U C_u$ energy distribution in design 4, the figure is from Khoj.	22
3.8	3D-model of the Guide vane: Design 1	23
3.9	3D-model of the Guide vane: Design 2	24
3.10	3D-model of the Stay vane: Design 1	25
4.1	View of the Main Dimensions tab in Khoj	28
4.2	View of the Axial View tab in Khoj	28
4.3	View of the Distributions tab in Khoj	29
4.4	View of the Radial View tab in Khoj	29
4.5	View of the Blade Thickness tab in Khoj	30
4.6	View of the Summary tab in Khoj	30
4.7	Making a quilt using streamlines from Khoj and Boundary Blend	31

4.8	Boundary Blend at leading edge and merging hub and ring	32
4.9	Drawing of the hub and shroud sections	32
4.10	How to make a "slice" of the hub	33
4.11	Drawings of hub in Creo	34
4.12	Finish hub from Design 4	34
4.13	Axial view of the ring sketch in Creo	35
4.14	Finish ring from Design 4	35
5.1	Model of the test pieces ordered	37
5.2	The test rig used for pull-out strength testing.	38
5.3	The figure are showing a 4mm pin attached to the test piece and with the Ensat S inserted.	39
5.4	Pull-out strength testing	40
6.1	Showing pull-out strength for Kerb Konus Ensats with different thread di- ameter in different plastic materials [9].	43
B.1	Price offer for a full set of runner vanes to the Tokke model runner	iv
B.2	Price offer for a couple of test vanes to the Tokke model runner	v
B.3	Price offer for test piece in SLS material DuraForm HST	vi
B.4	Price offer for test piece in SLS material DuraForm PA	vii
C.1	Material range at ARRK for SLS printing	ix
D.1	Axial view of the Tokke model runner	xiv
D.2	Drawing of the guide vane	xv
D.3	Guide vane torque for VKL-runner [1]	xvi
D.4	Drawing of the stay vane shapes	xvii
D.5	Drawing of the stay ring	xviii
E.1	Product info about Kerb Konus threaded inserts Ensats S	xx
E.2	Product info about Kerb Konus threaded inserts Ensats SK	xxi
E.3	Product info about Kerb Konus threaded inserts Ensats SI/SBI	xxii
E.4	Product information about the DIN 7 pins	xxiii

Nomenclature

Symbols

Symbol	Definition	Unit
A	Area	$[m^2]$
B	Vane height	$[m]$
D	Diameter	$[m]$
F	Force	$[N]$
g	Gravity	$[m/s^2]$
H	Head	$[m]$
h	Head	$[m]$
I_P	Polar moment of inertia	$[m^4]$
I_x	Moment of inertia	$[m^4]$
n	Rotational speed	$[RPM]$
M	Moment	$[m/s]$
P	Power	$[W]$
p	Pressure	$[Pa]$
Q	Flow rate	$[m^3/s]$
q	Load	$[N]$
R	Radius	$[m]$
r	Radius	$[m]$
T	Torque	$[Nm]$
t	Thickness	$[m]$
U	Peripheral velocity	$[m/s]$
W	Relative velocity	$[m/s]$
Z	Number of pole pairs, runner vanes, guide vanes	$[m/s]$

Greek Symbols

Symbol	Definition	Unit
α	Guide vane angle	[°]
β	Blade angle	[°]
η	Efficiency	[-]
ρ	Density	[kg/m^3]
Ω	Speed number	[-]
ω	Angular velocity	[rad/s]

Sub-Symbols

*	Refers to best efficiency point
<i>A</i>	Refers to available
<i>atm</i>	Atmospheric pressure
<i>e</i>	Refers to effective
<i>g</i>	Refers to guide vane
<i>h</i>	Refers to hydraulic
<i>m</i>	Refers to meridional direction
<i>max</i>	Refers to maximum value
<i>min</i>	Refers to minimum value
<i>P</i>	Refers to generator pole pairs
<i>R</i>	Refers to required
<i>r</i>	Refers to runner
<i>sv</i>	Refers to stay vanes
<i>u</i>	Refers to peripheral direction
<i>va</i>	Vapor
0	Refers to
1	Refers to runner inlet
2	Refers to runner outlet

Abbreviations

AM	=	Additive Manufacturing
BEP	=	Best Efficiency Point
CAD	=	Computer-Aided Design
CNC	=	Computer Numerical Control
FEM	=	Finite Element Methode
NPSH	=	Net Positive Suction Head
NTNU	=	Norwegian University of Science and Technology
OS	=	Operating System
PA	=	Polyamide
PTC	=	Parametric Technology Corporation
RPM	=	Revolutions Per Minute
SLS	=	Selective Laser Sintering
VKL	=	Vannkraftlaboratoriet (Waterpower Laboratory)

Chapter 1

Introduction

In Norway about 99% of all the electricity production is coming from hydropower. There are power plants all over the country, and a lot of them are built back in the 60s and 70s, the need for upgrading and replacing of old turbines is coming. The low electricity prices in Norway have made it hard for the energy producers to conduct new profitable development projects and larger maintenance project on old power plant. In order to keep the cost down, better and cheaper technologies and manufacturing methods need to be developed. To be able to do that a lot of research needs to be done.

When new development projects and larger maintenance projects are being conducted, a model turbine is often manufacture and model tests are conducted to find the best design for the prototype runner. Sometimes the industry uses the Waterpower laboratory at NTNU to run their model tests, and if they do not need the model afterwards they are giving it to NTNU. The Tokke model runner was given to NTNU from the industry.

1.1 Objectives

The main objectives for this thesis is come up with new mechanical designs of Francis model runners, guide vanes and stay vanes. The new designs should combined parts made by traditional manufacturing methods and new methods like rapid prototyping.

1.2 Background

Turbines and pumps consist of complex geometries that are expensive to manufacture. The production of model Francis turbines to be used in the Waterpower laboratory at NTNU is a lengthy and costly process. The arrival of rapid prototyping opens for new designs of pumps and turbine.

The Tokke model turbine and prototype have been the basis for the development of the new mechanical Francis model turbine design. The Tokke model test report with all the results from tests and drawings of the Francis model runner in the Waterpower laboratory, have been very helpful.

If the students at the Waterpower laboratory could have design their own turbine and test it in the laboratory, it would have been very educational for the student. But to be able to do that the manufacturing cost need to be significantly reduced.

Theory

2.1 High head Francis turbine design

A Francis turbine consists of a spiral casing, a set of stay vanes, a set of guide vanes and a runner see figure 2.1. When designing a Francis turbine it starts with the runner and then the guide vanes, stay vanes and spiral casing can be designed.

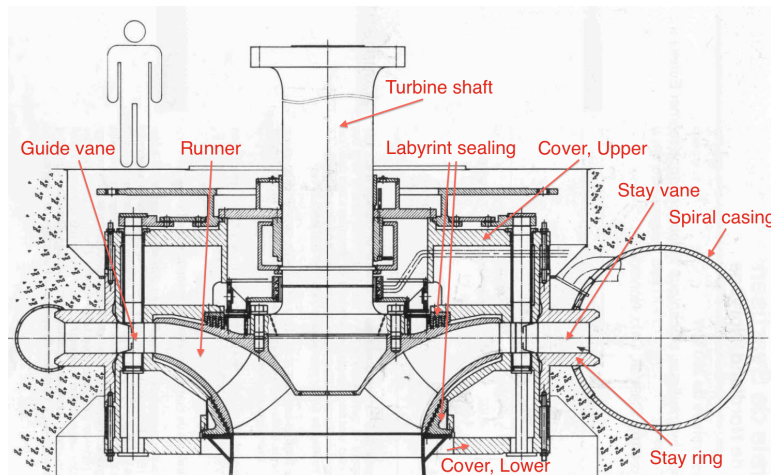


Figure 2.1: Axial view of high head Francis runner [12]

Francis runners are reaction turbines and there is a pressure difference from inlet to the outlet of the runner. At the runner inlet part of the specific energy is pressure energy. From the flow through the runner the specific energy is converted to mechanical energy partly from drop in pressure and partly from the impulse force due to changes in direction of the relative velocity. The turbine has to be completely filled with water to obtain the pressure drop through the runner and Francis turbines are therefore also known as full turbines.[2].

2.1.1 Main Dimensions

Designing a Francis runner starts with getting the hydraulic data from the power plant site, these are based on the topography and hydrology. From this data the total net head, H_n , total flow rate, Q . Then the next is to start dimensioning the outlet of the runner.

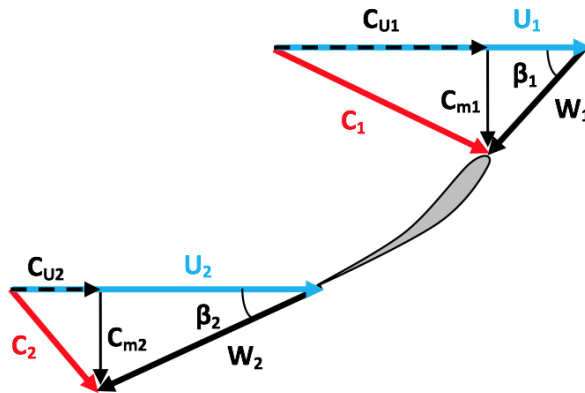


Figure 2.2: Velocity Triangles [10]

Notations used in the figure 2.2:

C	Absolute velocity	[m/s]
C_m	Meridian component of C	[m/s]
C_u	Tangential component of c	[m/s]
U	Peripheral velocity	[m/s]
W	Relative velocity	[m/s]
β	Angle between the relative and peripheral velocit	[°]
1	Inlet	[—]
2	Outlet	[—]

High head Francis turbines have an increasing difference between the inlet diameter and the outlet diameter for increasing net head.

Dimensions at runner outlet

The outlet is a critical point for cavitation, and it is appropriate to start the dimensioning at the outlet. First the peripheral velocity, U_2 , and the outlet angle, β_2 , are chosen from empirical data. The values can be found in the interval [2]:

$$15^\circ < \beta_2 < 22^\circ \quad (2.1)$$

$$32\text{m/s} < U_2 < 43\text{m/s} \quad (2.2)$$

The higher the velocity, U_2 , is, the higher head and the smaller the outlet angle, β_2 is, the higher head. When dimensioning the outlet it is assumed best efficiency point (BEP), and at BEP there is no swirl in the draft tube. It can then be assumed that:

$$C_{U_2} = 0 \quad [m/s] \quad (2.3)$$

Further C_{m2} is found by using the known values in the velocity triangles (figure 2.2), see equation 2.4.

$$C_{m2} = U_2 \cdot \tan \beta_2 \quad [m/s] \quad (2.4)$$

Now the outlet diameter, D_2 , can be found by using the relations between D_2 and C_{m2} , equation 2.5.

$$D_2 = \sqrt{\frac{4Q}{\pi C_{m2}}} \quad [m] \quad (2.5)$$

By knowing the outlet diameter, D_2 , the rotational speed, n , can be calculated using equation 2.6:

$$n = \frac{U_2 \cdot 60}{\pi D_2} \quad [RPM] \quad (2.6)$$

The number pole pairs in the generator, Z_P , depends on the rotational speed, n , and the grid frequency, f_{grid} . In Norway the grid frequency is $50Hz$ and the number of pole pairs is found by using equation 2.7.

$$Z_P = \frac{f_{grid} \cdot 60}{n} \quad [-] \quad (2.7)$$

There are requirements that the turbine need to have a synchronous rotational speed to be attached to a grid with constant frequency, and therefor the number of pole pairs, Z_P , has to be an integer. In order to get synchronous speed, the value of Z_P has to be round up or down. From the new Z_P the new corrected synchronous speed, n_{Corr} , is calculated. To keep the outlet blade angle, β_2 , for this geometry, a new corrected outlet diameter, $D_{2,Corr}$, is calculated from the synchronous speed [2].

Keeping flow rate, Q , and outlet angle, β_2 the same and $C_{U_2} = 0$ the new corrected and the old velocity triangle at the outlet will have geometric similarity, see figure 2.3.

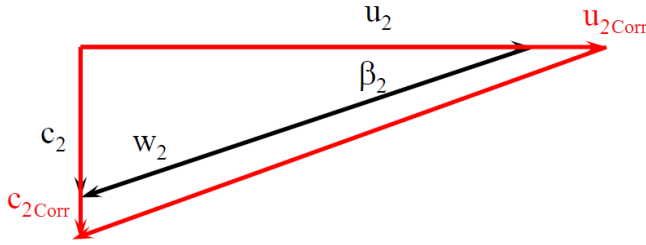


Figure 2.3: Velocity Triangles corrected [12]

$$\tan \beta_2 = \frac{C_{m2}}{U_2} = \frac{C_{m2,Corr}}{U_{2,Corr}} = \frac{\frac{4Q}{\pi D_2^2}}{\frac{\pi n D_2}{60}} = \frac{\frac{4Q}{\pi D_{2,Corr}^2}}{\frac{\pi n_{Corr} D_{2,Corr}}{60}} \quad [-] \quad (2.8)$$

Rearranging the equation 2.8 giving:

$$n_{Corr} D_{Corr}^3 = n D_2^3 \quad (2.9)$$

Now the new corrected outlet diameter, $D_{2,Corr}$, can be calculated using equation 2.10.

$$D_{2,Corr} = \sqrt[3]{\frac{n D_2^3}{n_{Corr}}} \quad [m] \quad (2.10)$$

Submerging

When designing high head Francis turbines the level of submergence need to be calculated. If the turbine is not sufficiently submerged cavitation may occur. To avoid cavitation the water pressure in the runner need to be higher than the vapor pressure. The level of submergence is expressed as Net Positive Suction Head (NPSH), and is found by using the equation 2.11.

$$NPSH_R = a \frac{C_{m2}^2}{2g} + b \frac{U_2^2}{2g} \quad [m] \quad (2.11)$$

The parameters a and b are depending on the speed number, Ω , and based on empirical data they are found in the interval [2]:

$$1.05 < a < 1.15 \quad (2.12)$$

$$0.05 < b < 0.15 \quad (2.13)$$

The speed number, Ω , are an dimensionless number that is an expression for the rotational speed at a given head at BEP, and it can be found from the equation 2.14:

$$\Omega = \underline{\omega} \cdot \sqrt{Q} \quad [-] \quad (2.14)$$

NPSH are dependent of the runner geometry and need to fulfill the following requierment to avoid cavitation:

$$NPSH_R < h_{atm} - h_{va} - H_S = NPSH_A \quad (2.15)$$

Using the Thoma cavitation number, σ , is an other method to calculate how much the turbine need to be submerged. The Thoma cavitation coefficient is found by calculating the speed number, Ω for the runner and then use the graph in figure 2.4 to get σ [12].

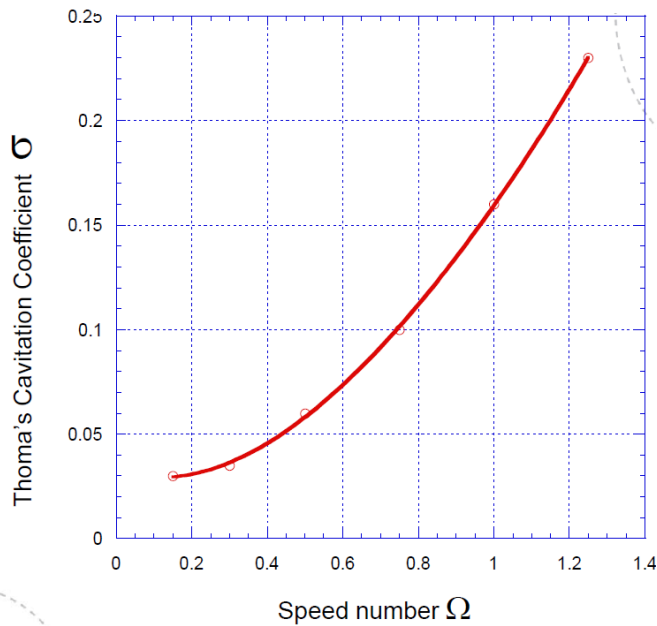


Figure 2.4: Thoma cavitation coefficient [12]

When σ is found, the level of submergence is calculated using the equation 2.16.

$$H_s < 10 - \sigma H_e \quad (2.16)$$

If the turbine not is sufficient submerged and there is not possible to move the turbine, then it is necessary reduce the rotational speed, n . Reducing n will need a generator with a larger numer of pole paris, Z_P , and due to that the size of the runner will increase.

Dimensions at runner inlet

When the dimensioning the inlet the inlet diameter, D_1 , inlet height, B_1 , and the inlet angle, β_1 are calculated. For the dimensioning of the inlet empirical values are needed. Reduced values are introduced in the design process, and they are indicated with a underline. The dimensioning starts with the Euler turbine equation:

$$\eta_h = \frac{U_1 C_{u1} - U_2 C_{u2}}{g H_e} \quad [-] \quad (2.17)$$

By introducing the reduced values and rearranging the equation 2.17, assuming BEP and no rotation in the outlet, $C_{u2} = 0$, the Euler equation is reduced to:

$$\eta_h = 2U_1 C_{u1} \quad [-] \quad (2.18)$$

The hydraulic efficiency, η_h , is normally set to $\eta_h = 0.96$. The relation between U_1 and C_{u1} are chosen to minimize losses by precussion. For high head Francis runner the reduced peripheral velocity, \underline{U}_1 in the range 0.71 – 0.73 will meet the requirement. The equation 2.18 is used to find C_{u1} and then the equation 2.19 is used to find U_1 [2].

$$U_1 = \underline{U}_1 \cdot \sqrt{2 \cdot g \cdot H_e} \quad [m/s] \quad (2.19)$$

Now the inlet diameter can be found using equation 2.20:

$$D_1 = \frac{2\underline{U}_1}{\underline{\omega}} = \frac{U_1 \cdot 60}{n \cdot \pi} \quad [m] \quad (2.20)$$

Using the velocity triangle (see figure 2.2) for the inlet, an expression for the inlet angle, β_1 , can be found.

$$\tan\beta_1 = \frac{C_{m1}}{U_1 - C_{u1}} \quad [-] \quad (2.21)$$

In order to calculate the inlet angle, β_1 , C_{m1} need to be found. Using the continuity equation is giving:

$$C_{m1} A_1 = C_{m2} A_2 \quad (2.22)$$

Based on experiences from turbine manufacturers in Norway, an acceleration of 10% through the runner are desirable. [2]. That gives:

$$C_{m2} = 1.1 \cdot C_{m1} \quad [m/s] \quad (2.23)$$

The inlet height, B_1 , can now be found using equation 2.24

$$B_1 = \frac{1.1 \cdot D_2^2}{4 \cdot D_1} \quad [m] \quad (2.24)$$

2.1.2 Energy Distributions

The energy distribution are showing how the energy is distributed along the blades through the runner. The distribution describes the transformation from pressure energy to rotational energy.

There is two ways to calculate the distribution, one way is to choose the $U \cdot C_u$ distribution, and calculate the β distribution. The other way is to choose β and then calculate $U \cdot C_u$ [8]. The calculations are done using the equation 2.25.

$$\beta = \arctan \frac{C_{m1}}{U_1 - C_{u1}} \quad [^\circ] \quad (2.25)$$

For high head Francis turbines, it is desirable to utilize most of the energy at a relatively large diameters. The blades are thickest at the leading edge to withstand the high tensions due to the large pressure differens. The blades becomes thinner towards the trailing edge due to lower pressurer differences and less tension. Avoiding a larege slip angle is desirable to reduce the risk for cavitation. For a good blade design, the C_u component in one point along a streamline should never be lager than the U component [5].

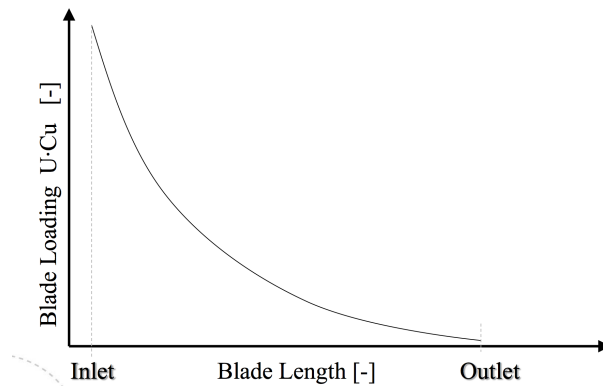


Figure 2.5: The figure are showing $U \cdot C_u$ blade loading from inlet to outlet [12].

2.1.3 Simplified calculations on a high head Francis runner

In a Francis runner the strength calculations is due to the complex geometries and load conditions very difficult to determine exactly. Therefore simplifications is necessary to be able to do some calculations.

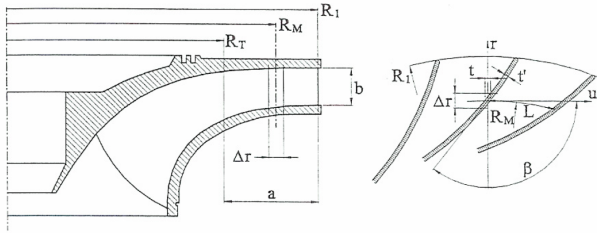


Figure 2.6: Principal sketch of high head Francis runner [3]

In high head Francis runners most of the torque are transmitted to the hub at relatively large diameters. For simplifying the calculations it is assumed that the whole torque is transformed outside R_T , see figure 2.6.

$$R_m = \frac{R_1 + R_T}{2}, \text{ and } a = R_1 - R_T \quad [m] \quad (2.26)$$

The load, Δp , can be calculated from the equation 2.27, by assuming the torque, M_r , is uniformly distributed on the runners inlet part, from R_T to the inlet.

$$M_r = Z a b R_m \Delta p = \frac{P}{\omega} \quad [Nm] \quad (2.27)$$

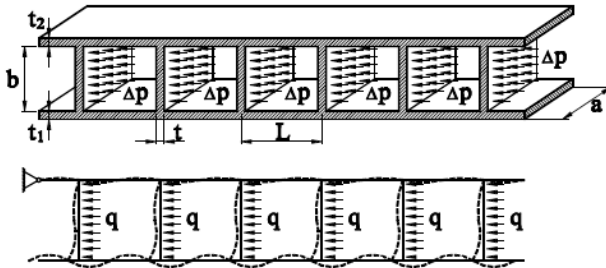


Figure 2.7: Model of runner for strength calculations [3].

Assuming that the pressure load, Δp , is uniformly distributed over a vane gives:

$$\Delta p = \frac{P}{Z a b R_m \omega} = \frac{30 P}{\pi Z a b R_m n} \quad [Pa] \quad (2.28)$$

The load, q , over an radiell extension, Δr , on the vane:

$$q = \Delta p \Delta r \quad [N/m] \quad (2.29)$$

From a simplified method for calculating bending stress it can be assumed that the stiffness of the hub and ring are very large compared to the vane. Assuming this the bending stress can be calculated using the formulas for a beam that is fixed at one end, see figure 2.8. The equation for the torque is then:

$$M = q \frac{b^2}{3} \quad [Nm] \quad (2.30)$$

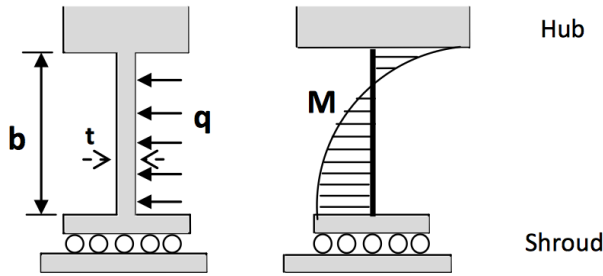


Figure 2.8: Principal sketch of high head Francis runner [3]

The maximum bending stress is then:

$$\sigma = \frac{M t}{I_z} \quad [Pa] \quad (2.31)$$

Where $I_z = \frac{\Delta r t^3}{12}$, and $t = \frac{t'}{\sin \beta}$ is the vane thickness in tangential direction. Inserting the equations 2.29 in the equation 2.30 and then into 2.31, the equation for maximum bending stress becomes:

$$\sigma = \frac{6 M}{\Delta r t^2} = \frac{2 b^2 \Delta p}{t^2} \quad [Pa] \quad (2.32)$$

This equation can be used to roughly give an approximation of the stresses in the runner.

2.2 Guide vanes

The guide vanes consist of a number of adjustable blades, they are adjusted to regulate the flow direction and the flow rate into the runner wheel. The guide vanes are adjusted with a servo motor that by the regulating ring, lever arms and links are turning the guide vanes into the desired position. The guide vanes also need to withstand the bending moment and the torque from the hydraulic forces [3].

To minimize the pressure pulsation due to the blade passing frequency, the number of guide vanes has to be chosen according to the equation 2.33 [8]

$$\frac{\text{Number of Guide vanes}}{\text{Number of Runner Vanes}} \neq \text{Integer} \quad (2.33)$$

The Francis model test rig on the Waterpowerlaboratory at NTNU has 28 guide vanes.

2.2.1 Hydraulic force acting on guide vanes

The hydraulic pressure after the guide vanes changes with the RPM of the runner and the pressure increases with increasing of RPM. The pressure upstream increases with decreasing guide vanes opening. The highest pressure acting on the guide vanes is when they are in closed position.

Guide vanes in closed position

The force acting on each guide vane when they are in closed position can be calculated using the following equations.

$$F_0 = \rho g H B_0 l = \frac{\pi \rho g H B_0 D_0}{z_0} [N] \quad (2.34)$$

The torque, T_0 , on the guide vane tap is then:

$$T_0 = F_0 \cdot a_0 = \frac{\pi \rho g H B_0 D_0 a_0}{z_0} [Nm] \quad (2.35)$$

The polar moment of inertia, I_P for the guide vane shaft:

$$I_P = \frac{\pi \cdot r^4}{2} [m^4] \quad (2.36)$$

The maximum shear stress, τ_{max} , due to torque can then be found:

$$\tau_{max} = -\tau_{max} = \frac{T_0}{I_P} \cdot r [Pa] \quad (2.37)$$

The stress in the transition between the shaft and the guide vane blade could be controlled by doing some estimate calculations :

$$\sigma_b = \frac{M \cdot r}{I_X} \quad [Pa] \quad (2.38)$$

The bending moment at the transition between the guide vane blade and the shaft can set as:

$$M = \frac{\pi \rho g H_0 B_0^2 D_0}{8 z_0} \quad [Nm] \quad (2.39)$$

The largest principal stress can be calculated by:

$$\sigma_{max} = \frac{\sigma_b}{2} \pm \sqrt{\frac{\sigma_b^2}{4} + \tau^2} \quad [Pa] \quad (2.40)$$

2.3 Stay ring and Stay vanes

The stay vanes are design to have no hydraulic effect, they have the main purpose of keeping the spiral casing together. The dimensions have to be given due to stress in the spiral casing.

2.4 CAD-Tool

During this thesis the CAD program PTC Creo Parametric 2.0 has been used to draw all the different designs of the runner vanes, guide vanes and stay vanes. The program is made by the computer software company Parametric Technology Corporation (PTC), which has specializing in 2D and 3D design software. The program PTC Creo was earlier known as Pro/Engineer. Creo Parametric runs on Microsoft Windows operating systems (OS) [13].

2.5 Design software - Khoj

The design software Khoj is a MATLAB program that was developed for designing Francis turbines. This program was developed by Kristin Gjørseter in her project and master thesis [8]. Khoj has been further improved by Peter Joachim Gogstad in co-operation with Gjørseter during his master thesis [10]. This design software has a graphical user interface (GUI) and this makes it easy to access all the different design parameters. For more details about how this program is working and how it was developed take a closer look at Gjørseter and Gogstad's master theses [8] [10].

2.6 Selective Laser Sintering - SLS

Selective Laser Sintering is a "3D-printing" method. The sintering process does not need any support structure during the build, because the unsintered powder surrounds and stabilised the part during the build process.

Laser sintering or selective laser sintering are terms that are used for printers that process plastic materials. There are many different material types from flexible "rubber like" materials to strong composite plastics. The types of materials vary from printer manufacture. The production method is commercialised by the U.S. company 3D Systems Inc. and the German company EOS GmbH.

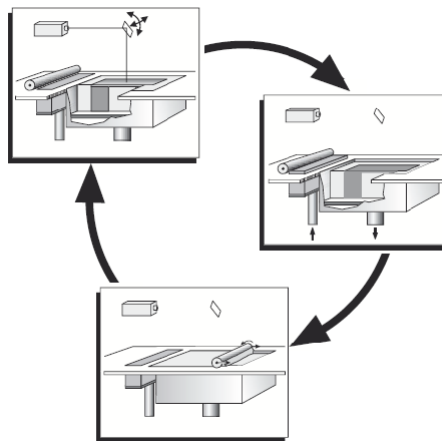


Figure 2.9: Laser sintering and laser melting; contouring and recoating process [7, p.41]

The technologies used in the machines from the two manufacturers are almost the same. The machines consist of a build chamber that is filled with powder with grain size smaller than $50\mu\text{m}$ and a laser unit on top that melts the contour of each layer in the X- and Y-direction. The build chamber is designed as a piston that can be adjusted in the Z-direction and after solidification of the contour of one layer the piston is moved down by one layer thickness. The space on the top of the powder is then filled with new powder that is ejected from a feed chamber by a roller. To spread the powder uniformly the roller rotates counter clockwise to its linear movement and the procedure of loading a new layer is often called recoating. An illustration of the process can be seen in figure 2.9. To minimise the power consumption of the laser and to avoid oxidation the build chamber is preheated and flooded by a shielding gas [7, p.40-42].

The layer thickness in SLS printers are normally around 0.1mm and therefore post-processing can be necessary to achieve a good surface quality. Sanding, coating or spray painting can do this. In Appendix C see figure C.1 a material data sheet for SLS material delivered by

Arrk Europe Ltd.

2.7 Rapid CNC Machining

Rapid CNC machining starts with a solid block in desired material, the CNC machine are removing material layer by layer until the shape of the model is finished. The machines are using 3D CAD data to make the pattern for machine; the pattern for each layer is the contour of the 3D model. It is almost exactly the opposite of 3D printing where the part is build layer by layer instead of removed. Since the machines are starting with a solid block of material, almost every possible materials could be chosen [6].

Protolab AS are using Arrk Europe Ltd as their manufacturer of prototypes. Arrk have their rapid CNC machines facilities in UK and the Far East. Arrk offers a range of machines with 5 and 3 axis capability and a wide range of standard materials [11].

2.8 Materials used in prototype and model turbines

Over the past decades the development of stronger and lighter materials, new production method, and new turbine designs have made the turbines larger, lighter and stronger. This has made it possible to utilize higher head for Francis turbines; now high head Francis runners are used where only Pelton turbines were used earlier. This sets high demands to the materials used. The turbine components have different requirements for materials due to different working environment.

In large high head prototype turbines the guide vanes and runner with labyrinth sealing are made of stainless steel, often steel grades such as $13Cr4Ni$ and $16Cr5Ni$. These parts can be exposed cavitation and erosion due to water flow with high velocity and therefore high quality steel is used [3].

In the Francis turbine rig on the Waterpower Laboratory at NTNU the runner hub and ring are made of Bronze JM-7 and runner vanes are made of Bronze JM-3. The guide vanes are made of stainless steel SIS 2343 and the stay vanes are made of aluminum EN-AW 6082 [1].

The Bronze JM-7 alloy used in the model runner consist of 80% copper, 10% aluminum, 5% iron and 5% nickel. The Bronze JM-3 alloy used in the runner vanes is a mixture of 88% copper and 12% tin. The JM-3 alloy is a bit softer than the JM-7 and is therefore also used in the upper- and lower labyrinth sealing.

Mechanical turbine design

3.1 New mechanical design of model turbines

In this section different new mechanical design of Francis model runners, guide vanes and stay vanes are described. The designs are based on the Tokke model turbine at the Waterpower laboratory at NTNU and the Tokke prototype runner. All designs are made so they would fit the Francis model test rig at NTNU.

3.1.1 Francis model runner design

In these subsections four different runner designs are described. All the designs are combining old and new manufacturing methods and different types of material.

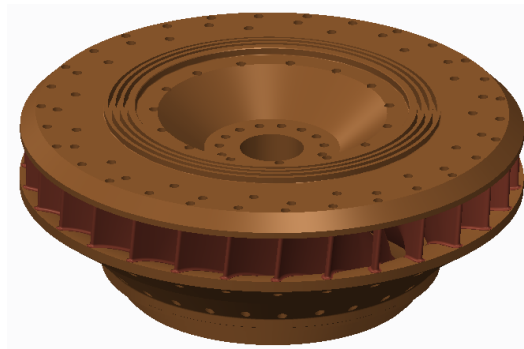


Figure 3.1: 3D-model of the Tokke model runner at NTNU

Runner and runner vanes Design 1

The first design considered was to use the existing Tokke turbine model, and just replaces the runner vanes with some made of a plastic material. The plan was to manufacture the runner vanes by rapid prototyping or rapid CNC machining. The Tokke model runner consists of 30 vanes, where 15 of the vanes are half-vanes and the other 15 are normal vanes.

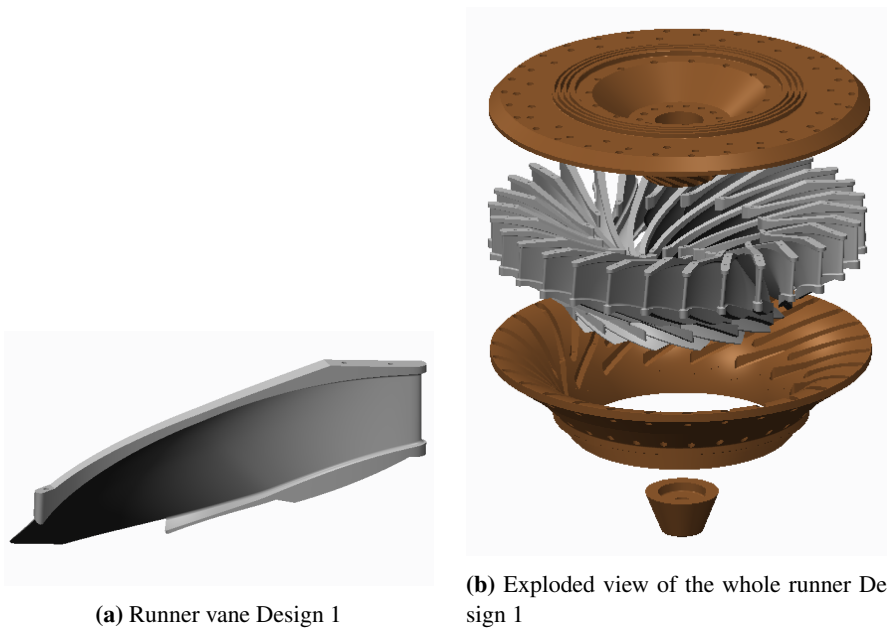


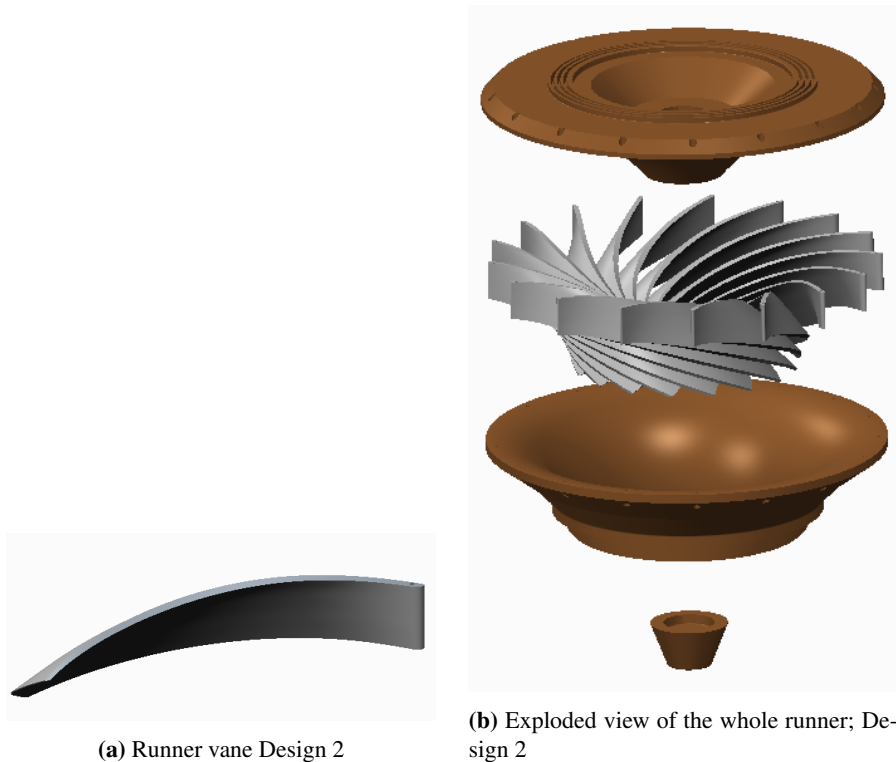
Figure 3.2: 3D-model of the Runner and runner vanes Design 1

To attach the parts together there were two alternatives; the first one is to produce the runner vanes with the existing holes a bit smaller and use self-tapping screws to attach it to the hub and ring. The second alternative is to make the holes bigger to insert self-tapping threaded inserts with internal M5 threads and use the existing M5 bolts to attach it to hub and ring.

The prototype company Protolab As in Trondheim was contacted to get a price estimate for manufacturing of all the 30 runner vanes. A price offer for manufacturing a couple of test vanes was also given. The price was given for SLS printing and using the PA plastic material DuraForm HST. The price offers can be seen in the figures B.1 and B.2 in the Appendix B.

Runner and runner vanes Design 2

The second design was to manufacture a new hub and ring out of bronze or stainless steel and the runner vanes of plastic. The runner is designed with 17 vanes, the same as the Tokke prototype runner. The shape of the blades is designed in Khoj, and is the same as Tokke. The hub and ring are made with a smooth surface with no grooves for the vanes, only holes at the leading edge for through bolts. The outside of the runner is made to fit the test rig at NTNU.



(a) Runner vane Design 2

(b) Exploded view of the whole runner; Design 2

Figure 3.3: 3D-model of the Runner and runner vanes Design 2

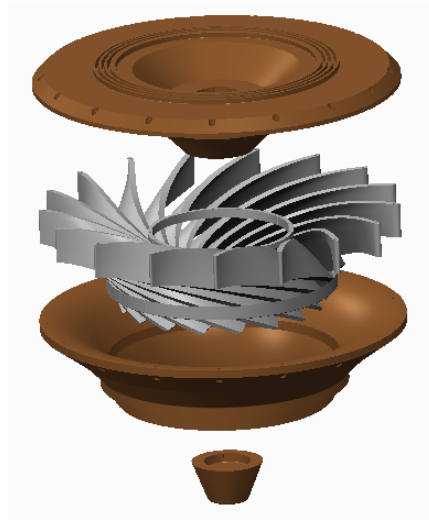
To hold the parts there will be a through bolt at the leading edge of the vanes and through the hub and ring. This will provide a good strength to hold the parts together. To attach the vanes to the hub and ring, it will be used glue and some small pins may be used to avoid slippage.

Runner and runner vanes Design 3

The third design is almost the same as the Design 2 but to get better support for the runner vanes a groove is machined around the hub and ring. All the runner vanes have a section that is $\frac{360}{17}$ and it will fit the groove and provide good support, see figure 3.4b.



(a) Runner vane Design 3



(b) Exploded view of the whole runner; Design 3

Figure 3.4: 3D-model of the Runner and runner vanes Design 3

To hold the parts together there will be used glue along the blades and in the grooves. In this case it would be enough to use pins on just a couple of vanes to avoid slippage because they are supporting each other.

Runner and runner vanes Design 4

The fourth and last design is to make the runner vanes as “slices” with a section of the hub and ring attached to it 3.5. The hub and ring should be made of stainless steel or bronze and the runner vanes of a plastic material. This way CNC milling would be used to manufacture the hub and ring and the runner vanes could be manufactured by SLS printing or by rapid CNC machining.

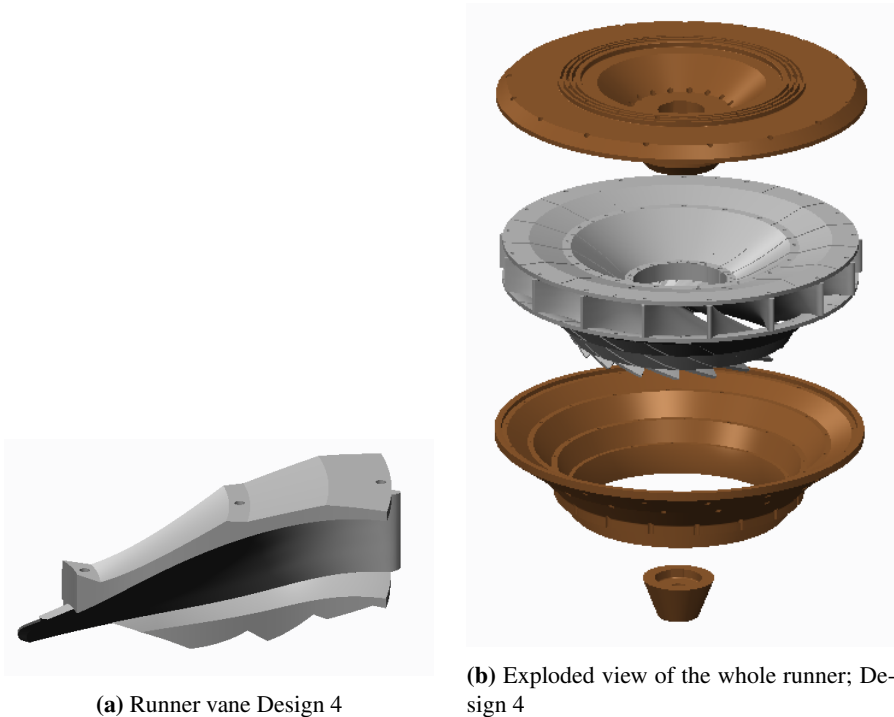


Figure 3.5: 3D-model of the Runner and runner vanes Design 4

To keep the runner together there are threaded rods at the leading edge with a threaded insert at the hub and ring side. The threaded inserts are screwed inside the hub and ring sections of the runner vanes, and they are mounted with a fixed distance between each other to keep a constant inlet height. At the ends of the threaded rods there are M5 nuts to tightening together the hub and ring, see figure 3.6.

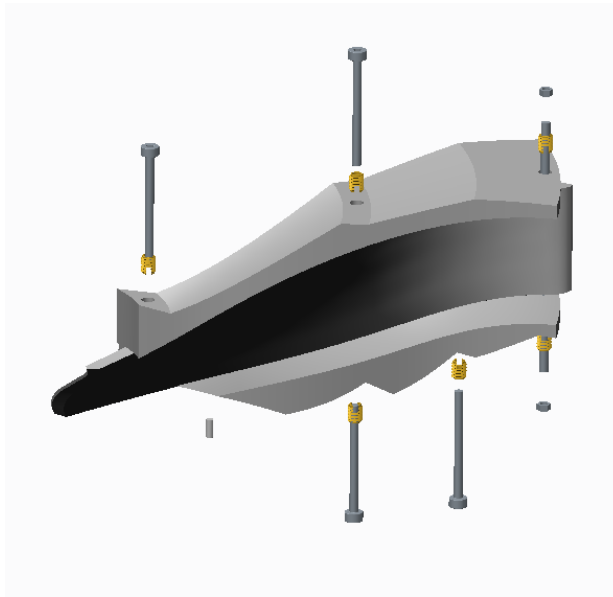


Figure 3.6: This figure show how the runner vanes in Design 4 will be attached to the hub and ring.

For this design a new blade shape was made. The new shape was designed by setting the $U \cdot C_u$ energy distributions to a linear distribution, where the energy is equally distributed along the blade. This was to get a unstable runner and try to provoke some vibrations [4]. The energy distribution can be seen in figure 3.7.

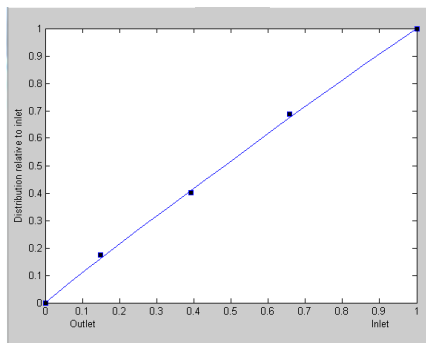


Figure 3.7: This figure shows the $U \cdot C_u$ energy distribution in design 4, the figure is from Khoj.

3.1.2 Guide vane design

In this section some new mechanical design of guide vanes are described. The goal was to come up with a new design that reduces the manufacturing and material cost.

Guide vane: Design 1

The first guide vane design is to manufacture the guide vane blade in a plastic material and the guide vane tap and shaft in stainless steel or bronze to keep a good strength and withstand the torque. The guide vane shaft and tap are produced with a "disc" at the end, with five holes. There are also five holes on the top and bottom of the guide vane blade; the holes are 3mm in diameter and 3mm deep. Inside the holes on the shaft and tap pins are glued, and then glued to the guide vane blade. These pins are used to make the guide vanes withstand the hydraulic force and torque acting from the water pressure.



Figure 3.8: 3D-model of the Guide vane: Design 1

Guide vane: Design 2

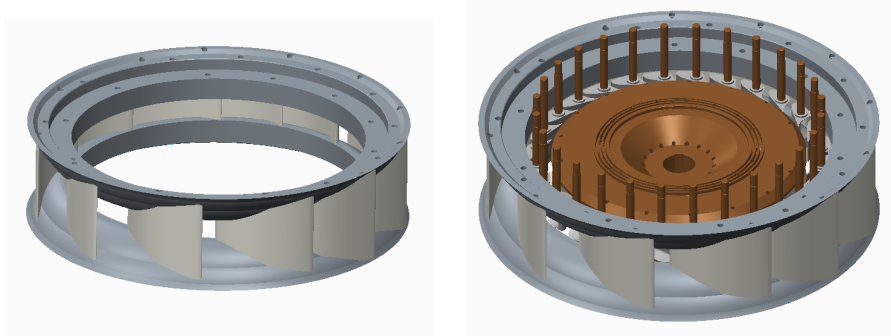
The second guide vane design is the same as Design 1 with plastic vane and steel shaft and tap, but here the "disc" that is a part of the shaft and tap in Design 1 is here a part of the vane. This is to make a stronger transition that is absorbing the forces from the water pressure. On the top and bottom of the vane there is a hole for the shaft and tap, and it is shaped almost like a keyhole, see figure 3.9a. The purpose of it is prevent the shaft and tap from spinning when the guide vanes are adjusted or when there is a torque acting on the guide vanes due to the flow.



Figure 3.9: 3D-model of the Guide vane: Design 2

3.1.3 Stay vane and stay ring design

In this section one alternative design of the stay ring and stay vanes are described.



(a) Stay vane Design 1

(b) Turbine with guide vanes and stay vanes

Figure 3.10: 3D-model of the Stay vane: Design 1

Stay vane: Design 1

The new mechanical design of the stay vanes have the same shape as the existing vanes in the Francis test rig at the Waterpower laboratory. Normally the vanes are welded to the spiral casing and the stay ring, and hold the spiral casing together. This design are using stay vanes made of plastic and welding will not be possible, therefore large steel bolts through the stay vanes, stay ring and the spiral casing will be used. There are threaded inserts at the top and bottom of the stay vanes to keep a constant inlet height on leading edge of the stay vanes and preventing the spiral casing from collapsing. To avoid leakage, the stay vanes are also glued to the stay ring as a sealing.

Chapter 4

Method

4.1 How to design a Francis runner to be used in the laboratory

In this section it is described how a Francis model runner can be designed by using the MATLAB program Khoj to get two sets of streamlines, one for the pressure side and one for the suction side. These streamlines are used to make a CAD model of the runner vane. The Tokke prototype runner was used as a reference design in Khoj and scaled down by a factor of 5.1 in Creo to get the size of the model runner.

Table 4.1: Input data from Tokk used in Khoj [4]

Tokke input data	
Head	$H = 377[m]$
Flow rate	$Q = 377[m^3/s]$
Number of pole pairs	$Z_P = 8$
Rotational speed	$n = 375[rpm]$
Inlet hight	$B_1 = 0.3[m]$
Outlet diameter	$D_2 = 1.78[m]$
Number of blades	17

This section describes how the model turbine in in Design 4 can be drawn.

4.1.1 Turbine design in MATLAB program Khoj

To star the program Khoj the file *RunMe.m* is run in MATLAB. After running the file Khoj will start and it is shown with a GUI that make it easy to use. In the *Intro* tab it is possible to choose between starting a new project, load an earlier project or compare with CFX. To make a new design just push the *New Project* button and select the tab *Main Dimensions*.

Main Dimensions

In the graphical view of the *Main Dimension* tab the main dimension of the turbine is inserted, see figure 4.1. Here the values for Head, H , Flow, Q , number of pole pair in generator, Z_p , outlet diameter, D_2 , inlet height, B_1 and reduced inlet peripheral velocity, U_1 is submitted. The reduced inlet peripheral velocity is changed by sliding the bar, see figure 4.1. The velocity triangles for inlet and outlet is shown in *Main Dimensions* and they are changing by changing values.

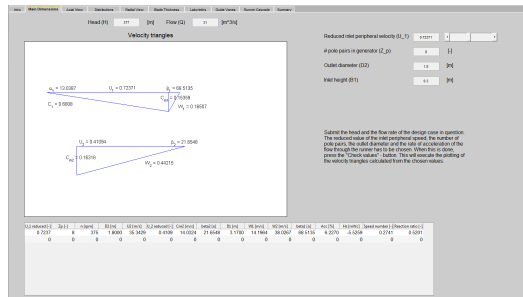


Figure 4.1: View of the Main Dimensions tab in Khoj

Axial View

In the graphical view of the *Axial View* tab the axial view of the streamlines are shown. Here the number of streamlines is chosen, the height difference from the leading edge to the trailing edge is set, b . There is four control points with X and Y coordinates to adjust the shroud line data, and four points to adjust the trailing edge. This point can be changed by typing in the X and Y values for the points or by moving the points around, see figure 4.2. There are also two tab for resetting changes on the trailing edge or the shroud line. If the streamlines will be used to make a 3D-model the number of lines should be less than ten to get a smooth surface of the runner vanes.

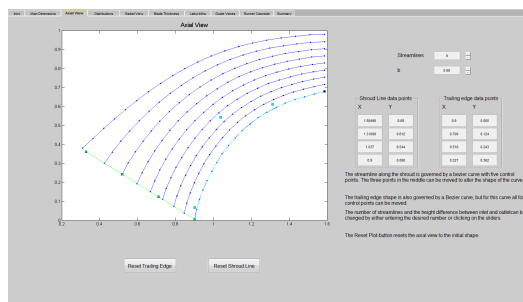


Figure 4.2: View of the Axial View tab in Khoj

Distributions

In the graphical view of the *Distributions* tab the energy distributions on the runner vane is shown. There is possible to choose between $U \cdot C_u$ distribution and Beta, β distribution. The distributions can be changed by moving the three points around, see figure 4.3.

In this case the $U \cdot C_u$ distribution was chosen and the distribution line was set to be an almost linear line, see figure 4.3. This was to get a model with runner vanes that may create vibrations. The distribution shown is from the Francis runner vane: Design 4.

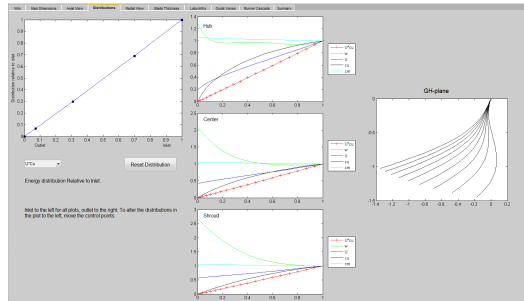


Figure 4.3: View of the Distributions tab in Khoj

Radial View

In the graphical view of the *Radial View* tab the blade leaning is set by moving three points on the graph up in the left corner. The number of runner blades is chosen by typing in the number up in the right corner, see figure 4.4. A radial view of the blade is also shown and it is possible to change what the figures on the right side are showing by choosing on the drop menu *Colormap an blades*.

In this case the number of blades was set to 17, the same as the Tokke prototype runner. The blade leaning was set to zero degrees to be able to have through bolts at the leading edge.

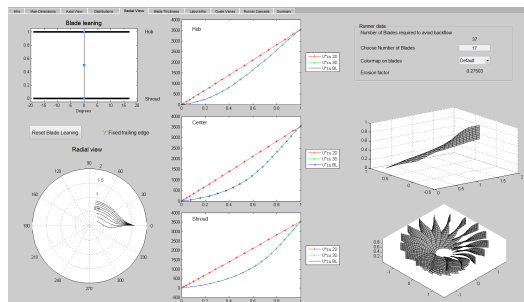


Figure 4.4: View of the Radial View tab in Khoj

Blade Thickness

In the graphical view of the *Blade Thickness* tab the blade thickness at leading edge and trailing edge are set, and the shape of the leading edge geometry are chosen.

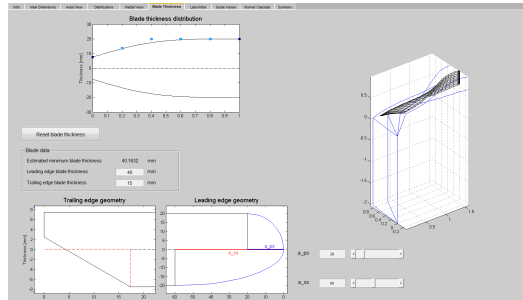


Figure 4.5: View of the Blade Thickness tab in Khoj

Summary

In the last tab *Summary* an table with overview of all the velocity components, characteristic parameters and the turbine dimensions are shown, see figure 4.6.

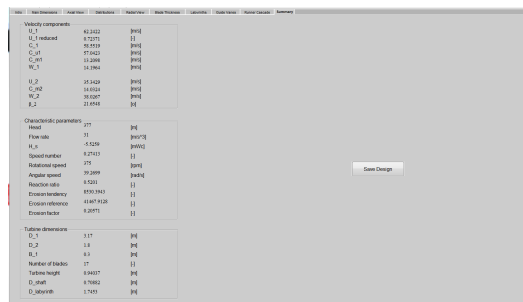


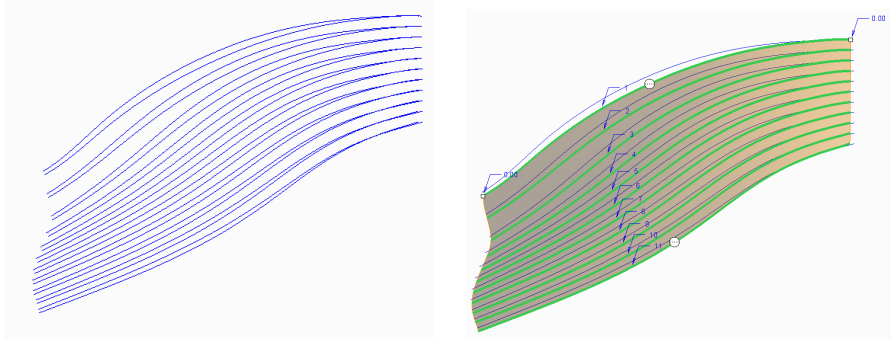
Figure 4.6: View of the Summary tab in Khoj

In the GUI in Khoj there is also a tabs for the *Labyrinths*, the *Guide Vanes* and one for the *Runner Cascade*. In this case nothing were changed in these tabs because the guide vane profile from Khoj are not the same type as the one on the Francis test rig at the Waterpower Laboratory. The only thing used from Khoj is the shape of the runner blade.

4.1.2 Drawing of a Francis runner vane in Creo Parametric

In this section it will be described how to draw a 3D-model of a Francis runner vane in the CAD program Creo Parametric (Pro/Engineer). The focus of this section will be how to draw a runner vane ("Slice") like the one described in the section *Design 4*.

1. Import the following curve files from Khoj; bladess.ibl and bladesps.ibl. This files contains a set of streamlines for the pressure- and the suction side of the runner vane. See figure 4.7a



(a) Streamlines imported from Khoj

(b) Boundary Blend between the streamlines

Figure 4.7: Making a quilt using streamlines from Khoj and Boundary Blend

2. If the streamlines is not oriented the way that is desired, a new coordinate system can be made. This is done by using the function *Coordinate System*, then select the existing coordinate system as *References* just by click on it in the left menu. Now the new *Coordinate System* can be oriented by selecting the *Orientation* tab and then rotate it about one of the coordinate axis. In this thesis the runner vanes is drawn in a *Coordinate System* that is rotated -90° about the X-axis.
3. Use *Boundary Blend* between the curves from bladesps.ibl to make a quilt at the pressure side see figure 4.7b, repeat for the suction side. (If the thickness of the vane is wants to be changed, it can be done by *Offset* the two quilts).
4. Select the leading edge on the suction side and use the function *Extend* and remove $3 \cdot r$. Repeat the procedure on the pressure side and remove $1 \cdot r$.
5. Create the leading edge by using *Boundary Blend* between the pressure- and the suction side. Select *Constraints* and set *Conditions* to *Tangent* and set the *stretch Value* to 3 for suction side and 1 for the pressure side see figure 4.8a.
6. Use *Boundary Blend* the edges of the pressure- and suction side at the trailing edge.
7. Select the suction side edge and use *Extend* to remove $\frac{2}{3}$ of the thickness towards the pressure side. Then select the quilt edge on the suction side and use *Extend* to remove $\frac{2}{3 \cdot \sin 30} \cdot thickness$. Then use *Boundary Blend* to close the gap.

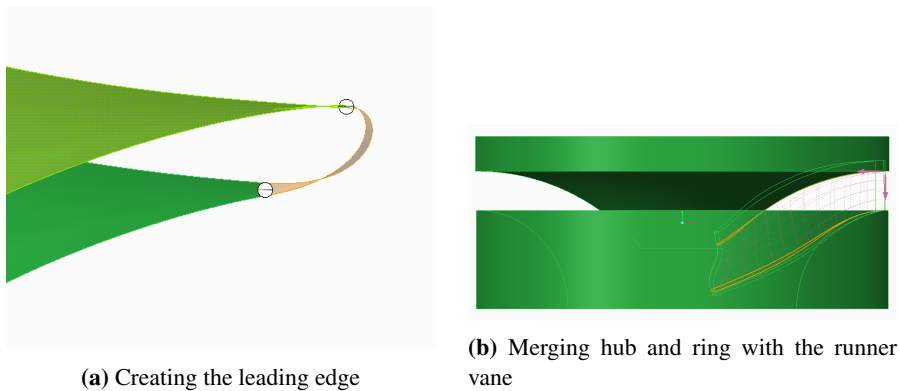


Figure 4.8: Boundary Blend at leading edge and merging hub and ring

8. Use the function *Merge* to merge all the 5 quilts together.
9. Close the vane by make some *Boundary Blend* between the pressure- and the suction side at the top and bottom of the vane. The use the *Merge* function and merge all the quilts together.
10. Select the last Merge in the list to the left and use the function *Solidify* to solidify the vane.
11. Start a *Sketch* in the *Front Plane* and draw the left side of the axial view of the runner hub and ring. Make sure to extend the sketch so it cuts off the top of the vane. Exit the sketch and use *Revolve* around the center axis and select the tab *Revolve as surface*.
12. Select the hub and ring surfaces and use *Merge* and select *Options* tab and use *Intersect*. This way the surfaces cutting the hub and ring will close the vane and the rest of the hub and ring surfaces will be cut away. See the area inside the orange lines in figure 4.8b

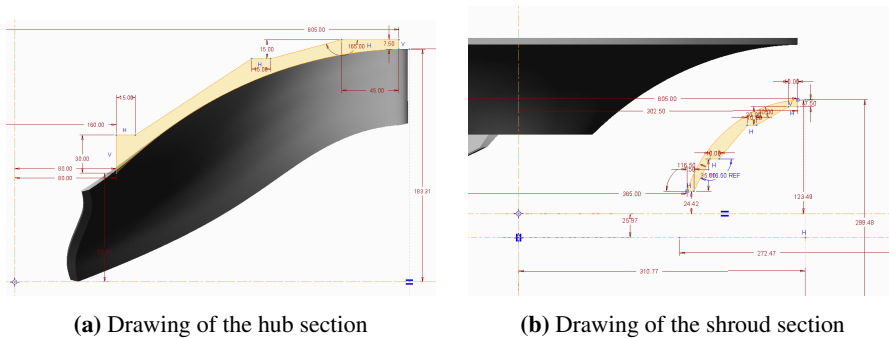


Figure 4.9: Drawing of the hub and shroud sections

13. Select the last *Merge* and use *Solidify* to make the runner vane a solid part.
14. Then start a *Sketch* in the *Front Plane* and draw the hub section of the runner vanes, see figure 4.9a. When the sketch is finish use *Revolve*, and revolve the section around the center axis.
15. To make the ring section start a *Sketch* in the *Left Plane* and draw the section, see figure 4.9b. Then repeat the same procedure as for the hub section.
16. Make a *Plane* and *Offset* it 300mm up from the *Top Plane*. Start a sketch in the new Plane and use *Project* on the outer edge of the hub and the edges on hub side of the runner vane. Then use *Construction Mode* and make a *Line* along the center of the vane. Then use the function *Rotate Resize* and rotate the centerline $\frac{360}{32}$ in each direction. Connect these two lines with the outer edge of the hub by using *Line* and make a tangent from the line edges to the hub line. Close the lines like figure 4.10a and exit the *Sketch*. Select *Extrude* and use the tab *Remove Material*. Select *Extrude to intersect with selected surface* and select the inner surface of the hub. This section is now a "slice" that is $\frac{1}{17}$ of the hub, see figure 4.10b. Make new *Plane* 300mm *Offset* from the *Top Plane* in the opposite direction and repeat the procedure for the ring side.

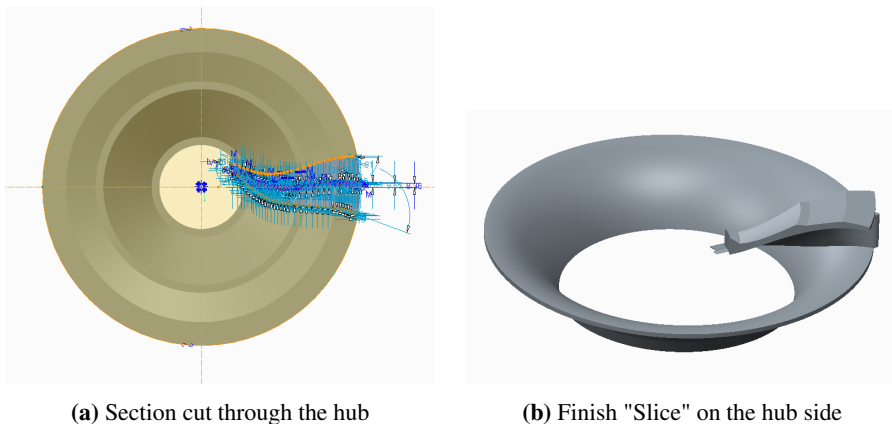


Figure 4.10: How to make a "slice" of the hub

17. Now the runner vane ("slice") is completed. Then make the holes for attachment, the holes are made in the center of each ledges. The three holes on the top of the vane for Ensats insert have a diameter from 7.3-7.5mm, see data sheet for Ensats figure E.1 in appendix E. At the trailing edge side of the ring sectin ther is a hole for DIN 7 pin $\varnothing 4$ mm, and ther three other holes on ring side er the same at for the hub section. At the leading edge there is a $\varnothing 5$ mm hole through for the M5 threaded rod.

4.1.3 Drawing hub and ring in Creo Parametric

Hub

1. Start a *Sketch* in the *Front Plane* and draw the hub as shown in the Tokke model drawing, see figure D.1 in Appendix D. Then to make the runner vanes fit, the hub section of the vanes needed to be removed from the hub, see figure 4.11a. Exit the sketch and use *Revolve* around the center axis.

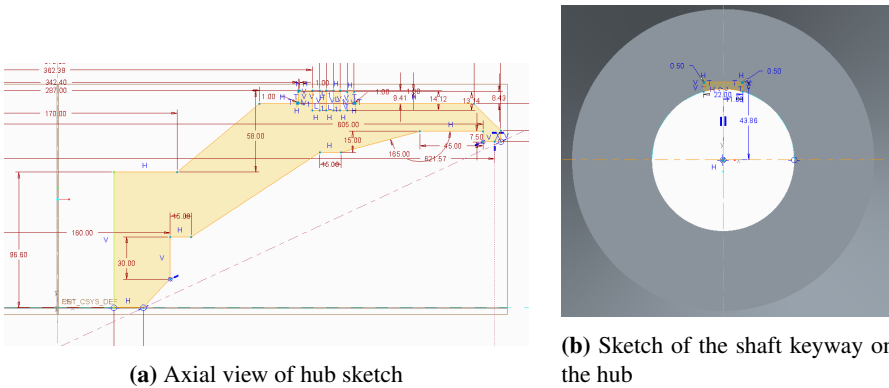


Figure 4.11: Drawings of hub in Creo

2. The next is make the keyway by starting a *Sketch* on the top of the hub and draw the keyway, see figure 4.11b. Then exit the sketch and *Extrude* a cut all the way trough the hub.
3. The holes for attachment are made by using the same distances from the center axis that was used for the runner vanes. The holes for bolts are made with countersink for the bolt head. When the holes for one vane are made, *Geometry Pattern* are used and an pattern of 17 for all the vanes are made 360° around the center axis.

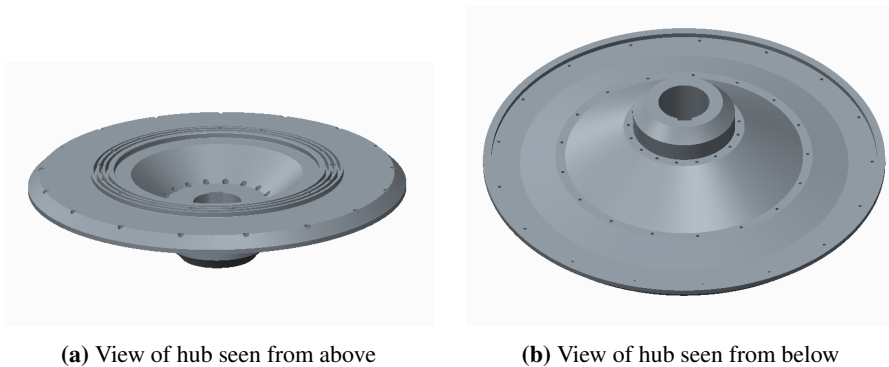
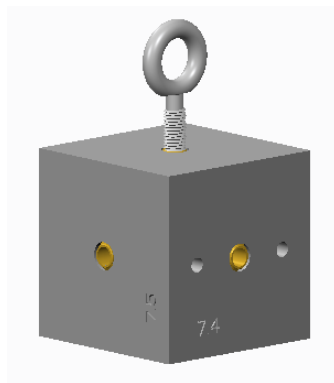


Figure 4.12: Finish hub from Design 4

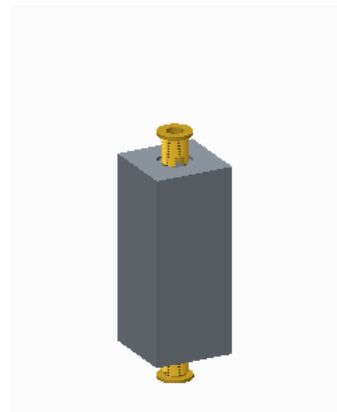
Experiment

5.1 Material tests

To find out if the polyamide (PA) material DuraForm HST-SLS from Arrk Europe Ltd. has good enough strength to hold the runner hub and ring together with Ensaf threaded inserts, pins and M5 bolts, some test need to be done. Two test pieces were drawn in Creo and then ordered from Protolab As to test the strength of the material. The two pieces were produced by SLS printing and one of them was sprayed with some coating to show how a smoother surface could be achieved, the test pieces are shown in figure 5.1.



(a) The test piece for pull-out strength and torque testing



(b) The test piece for the compression test

Figure 5.1: Model of the test pieces ordered

5.1.1 Test 1: Pull-out strength test

The Ensats S threaded inserts were mounted into the cube test piece by using a homemade installation tool. The tool was a M5 bolt, where the head was cut off, then two nuts and a washer was screwed on and the Ensats S. The tool was mounted in a drill press, and the inserts were screwed into the test piece by turning the chucks with one hand and gently push down the drill press with the other hand.

To be able to test the SLS material piece with the Kerb Konus Ensats S self-tapping threaded inserts a test rig was made. The test rig was made of a square beam that was approximate 550-650mm long. At the end of the beam a square plate was welded to hold the test piece, and in the center of the plate a 18mm hole was drilled. At the opposite end a threaded rod was bent into a hoop and welded to the beam to be able to hang it up in a pulley. On one side of the beam a square hole was cut to be able to place the test piece into the rig. The test rig can be seen in figure 5.2.

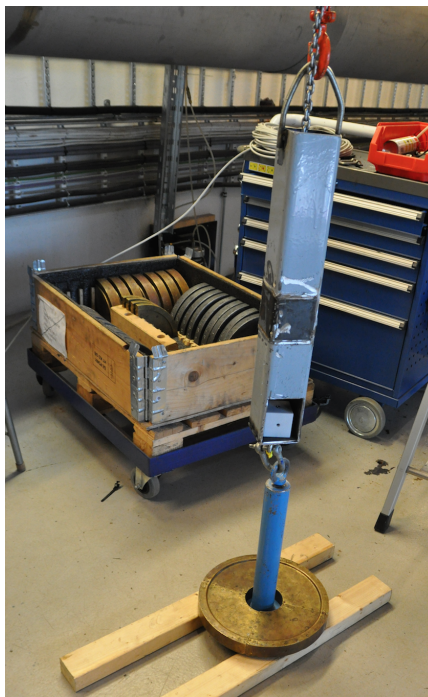


Figure 5.2: The test rig used for pull-out strength testing.

To be able to load weight on the test rig was hung up in a pulley, and a M8 nut was welded to a M5 bolt, then a M8 eyebolt was screwed into the nut and fasten to the test piece. In the eyebolt a shackle was attached and the weight "disc" for the generator torque calibration was used to load weights, see figure 5.2.

5.1.2 Test 2: Compression test

In order to find out if a threaded rod with threaded inserts in the hub and ring section of the runner vane, are enough to keep a constant inlet height, a compression test need to be done. The test can be done by using the test piece seen in figure 5.1b, one threaded insert at each end and a threaded rod through. Then measure the distance between the two inserts and put the piece into a hydraulic press. The load added need to be measured and the distance between the inserts. The objective is to find out how much load in can handle before the distance is changed.

5.1.3 Test 3: Torque test

A pin would be used to attach the runner vanes to the ring and need to be tested. The cube test piece used in the pull-out strength test, was also design to be used for the torque test. At one side of the cube there was made two holes that are 4mm in diameter, and are made to fit a $\varnothing 4\text{mm}$ pin. To test the torque a pin is inserted in one of the two holes and a Ensaf S is mounted in the 7.4mm center hole, see figure 5.3. The next is to use a steel plate with one 4mm hole for the pin and one hole for a bolt. The test piece is placed on the plate and the bolt is screw into the Ensaf S and tightens to the plate. Then the plate is attached to something heavy that not will move and the test piece are exposed to a torque until the pin or the plastic breaks. The force needed before it breaks is then measured.

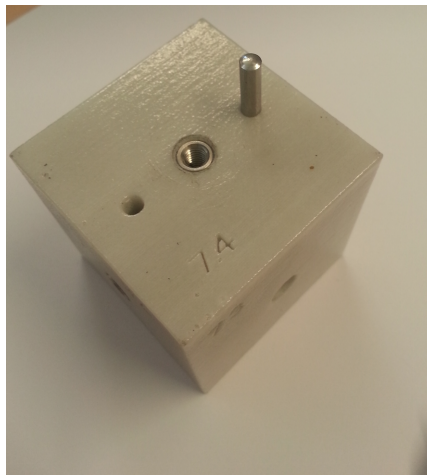


Figure 5.3: The figure are showing a 4mm pin attached to the test piece and with the Ensaf S inserted.

5.2 Results from material tests

Due to lack of time and not having all the equipment needed, only the pull-out strength test was done.

When testing the pull-out strength it started with the thread inserts in 7.5mm holes, then the 7.4mm holes. For the two 7.5mm holes and the first of the 7.4mm holes, 160 kg was loaded onto the disc before the Ensaf S inserts were pulled out. For the next 7.4mm hole all the calibration weights was used (about 230kg) and it was still not enough to pull it out. To gain more weight scrap metal were weighed and used as weights, after loading all the scrap metal that it was room for, the total weight was up in about 330kg, see figure 5.4a.



(a) Loading with scrap metal to gain weight



(b) Using a crane weight to measure the load

Figure 5.4: Pull-out strength testing

After all the metal scrap was used, a new method had to be used. Then a crane weight was borrowed on the Thermal Energy workshop, the crane weight had a limit of 500kg. The limit was reached without problem. After that there was not found any measuring equipment with a higher limit, therefore the maximum pull-out force was not found. The two 7.3mm holes was either not tested, and they would probably withstand even more than the 7.4mm hole.

Discussion

6.1 The new runner and runner vane designs

The first alternative considered was the Francis Design 1 where the existing Tokke model runner hub and ring are being used, and replacing the runner vanes with someone made of plastic. This solution is a very good alternative when it comes to testing if the strength and stiffness in the material is good enough, but this gives small or almost no opportunities to change the design of the runner vanes. There is no trough bolts at the inlet and the plastic vanes are the only structure keeping the distance between the hub and ring. If the stiffness and strength in the plastic are not sufficient to keep a constant distance between the hub and ring the lower labyrinth sealing could touch each other and lose a lot of energy due to friction. This could also lead to leakage in the labyrinth sealing.

The second alternative with new hub and ring in bronze and runner vanes in plastic. This alternative has a trough bolt at the inlet, glue along the blades and pins to hold the parts together and lock it in place. The third alternative is almost the same as the second one, only with a groove around hub and ring, and a section of the hub and ring on the runner vanes. This sections will prevent slippage and give better support for the vanes since the vanes are supporting each other. Both design 2 and 3 may become unstable due to poor attachment, with only proper mounting at the leading edge, this would probably not be enough keep the runner firmly in place.

The last alternative considered is the Design 4 where the runner vanes have a section of the hub and ring. This alternative with the large sections is having a lot of possibilities when it comes to fixing. With all the fixings, it should be enough to keep the runner in place. The disadvantages with this are that the volume of the vanes is quiet large, and that increases the production cost, espically with SLS printing.

With the design 4 the hub and ring could be used for different design just by replacing the “slices”. It may be necessary to replace some of the holes to attach all the parts together. This way a new model runner with different vanes could be made only by changing the design of the vanes and make it fit the hub and ring.

The blade shape in design where the $U C_u$ energy distribution was set to be almost linear from inlet to outlet. This was made provoke some vibrations in the runner. The relative velocity, W , at the hub side was going up and down through the runner, and close to the trailing edge the velocity increases up 1.4 times the inlet velocity. On the center of the blade the relative velocity is almost constant the first $\frac{3}{4}$ of the blade length and the $\frac{1}{4}$ of the blade the velocity increases to over 2 times the inlet velocity. At the shroud side of the blade the velocity is constant the first half of the length and increases to almost 3 times the inlet velocity over the second half of the blade. For a blade that is designed good, the C_u component should never be larger than the U component, at the hub side of this design the C_u component is larger than U along the whole blade.

6.2 The new guide vane and stay vane designs

The first guide vane alternative was the one with a "disc" and pins and where the guide vane shaft and tap are glued to the guide vane blades. With this alternative all the forces and torque would be absorbed in the transition between shaft and the blade, and this is the weakest point.

The second guide vane with connection between shaft and blade almost like a keyhole. In this design the blade in would absorb all the forces and bending moment from the water pressure and the transition between shaft and blade only need to withstand the torque.

The during the Tokke model test at the Waterpower laboratory most of the tests was run with head, $H = 30 \text{ m}$, and rotational speed, $n = 540 \text{ RPM}$. According to the test results the maximum torque on the guide vanes was at approximate 1° opening and then the torque was just over 4 Nm , see figure D.3 in appendix D. According to some simple calculations done, the torque in closed position is about 15 Nm and the bending stress was calculated to about 38 MP . Due to this the new guide vane design at least need to withstand 15 Nm torque. The calculations could be seen in Appendix A.

The new stay vane design where plastic vanes and trough bolts are replacing the aluminum vanes welded to the spiral casing would probably not be economically profitable. That is because the shape of the stay vanes are not that complex and there are probably small differences from making the vanes of plastic by rapid prototyping, or standard material and production method.

6.3 Manufacturing methods and materials

The two rapid prototyping methods considered for manufacturing the parts for the new designs are selective laser sintering (SLS) and rapid CNC machining. Both methods have advantages and disadvantages.

Using SLS gives possibilities for more complex designs and with internal structures, such as channels for wiring and grooves for sensors. One of the disadvantages with SLS is that tolerance is not that good. When ordering SLS printed parts from Protolab AS and Arrk Europe there are four different plastic materials to choose between, see figure 2.9.

When using rapid CNC machining the quantity has a grate influence on the manufacturing price. If there is a production series of only a couple of parts the rapid CNC machining can not compete with SLS printing when it comes to price., but when there are larger series and large volume the CNC may be the cheapest method [6]. CNC machining from Arrk Europe gives a lot of different materials to choose from, there are over 35 standard materials and if thats is not enough other materials can be ordered [11].

Most of plastic materials used in rapid prototype machines could absorb a small amount of water, even if it are just 0.05% that could be enough to change the distance between the hub and ring with a tenths of a millimeter. The tolerance is so fine that this could be enough to make the labyrinth sealing and runner to touch and loose efficiency due to friction, and therefore is it important to have a design where the vanes not are able to move.

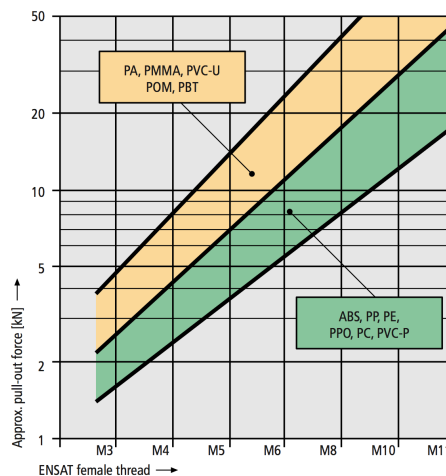


Figure 6.1: Showing pull-out strength for Kerb Konus Ensats with different thread diameter in different plastic materials [9].

When testing the SLS material and threaded inserts for pull-out force, there was some quiet large differences in the force for the same hole diameter. That could be due to not a perfect mounting of the inserts or because of roughness in the holes. According to the manufacturer the threaded insert Ensat with M5 internal threads should hold a pull-out force of approximate 10kN in PA plastic, see figure 6.1. That may be correct, because the Ensat in the 7.4mm was loaded with 500kg without giving any sign of giving in.

6.4 Production of runner blades and model test

In the start of this semester the plan was to produce new runner blades for a Francis model turbine and run model tests if they were available before end of the semester. Everything did not go as planned and due to lack of time and money the runner vanes was not manufactured. There was no available time in the laboratory before the end of May, and therefore it would not have been time to run model tests even if the runner vanes were manufactured.

6.5 FEM analysis of the new runner design

At the beginning it was planned to do an Finite Element Method (FEM) analysis of the new runner vane and guide vane designs to compare the results with empirical data and some simplified calculations done on the runner vanes and guide vanes. This was not done since there was not sufficient time.

Conclusion

7.1 Conclusion

It is possible to reduce the production time and cost of production of Francis model turbines, by combining new and old production methods.

Comparing the four different designs of the Francis runner vanes, the Design 4 is the best alternative both when it comes to strength and possibilities to change the design. The quiet large section of each vane gives better fixing opportunities and is more stable the other.

The guide vane Design 2 are the best alternative because in this design the vane with the "discs" is one solid part, and are absorbing all the bending moment from the water pressure. The connections between the vane, the guide vane shaft and tap only need to withstand the torque. That should not be any problem, but the connections could be reinforced with some steel bushings.

To change the stay vane design, and replace the vanes with someone made of plastic with trough bolt would probably not be a very good solution, that is because the production cost probably will be higher than for a regular method. It is also a risk of leakage under and over the vanes.

When it comes to manufacturing methods Selective laser sintering (SLS) would be the best method for producing the runner vanes, especially when the geometries are complex, that is because the support from the unsintered powder surrounding the part during build. If the runner vanes are designed with channels for wiring inside the blades and grooves for sensor, SLS printing is the only method. All parts with requirement to tolerance produced by SLS printing, need to be coated to get a smooth surface finish. The CNC machining are giving a smoother surface finish, so if the production cost is lower for CNC than SLS, then CNC should be used.

The runner vanes are produce with SLS printing or CNC and guide vanes and stay vanes are manufactured by CNC machining as long as they are not designed with slots for sensors or channels for wiring, then they are also SLS printed.

The hub and ring will be produced with standard CNC milling by a Norwegian mechanical workshop. These parts should be produced in bronze-JM7, the same material as the Tokke model runner hub and ring are made of.

If the Kerb Konus self-tapping threaded inserts are used to attach the runner vanes to the hub and ring, they must be properly installed. If they are not properly installed, they may not withstand the pull-out force needed, and therefore proper installation tools should be used.

Further Work

8.1 Further Work

As further work a FEM analysis of the new runner vane and guide vane designs could be done to control if they will withstand the forces from the water pressure in the Waterpower Laboratory Francis rig. The analysis should control for both the highest torque in open position and the highest force acting on the guide vanes when they are in closed position.

Continue the runner design process and do the changes needed before the runner vanes are ready to be manufactured. Manufacture the runner vanes, new hub and ring. Assemble the parts and run some model test in the rig at the Waterpower laboratory at NTNU.

Another possibility for further work could be to design a runner vane for testing with strain gage. It could be designed with a channel for wiring inside the blade and up through the hub. The vane could be designed with a groove for the strain gage so it not disrupts the flow. Just to test this method a runner vane for existing Tokke model runner could be made in plastic with channel for the wiring and replace one of the bronze vane.

As a start just to test the guide vane design, just a couple of existing guide vanes could be replaced with the new design. To control the new guide vanes a channel for wiring and a groove for strain gage could be added in the 3D-model before production.

Use the two test pieces and do the torque test and the compression test, described in the Experiment chapter. This is to find out if the fixing and material are strong enough.

As further work different plastic material could be analysed to see if there is some materials that are scalable compare to the different stainless steel grades used in prototype runners.

Bibliography

- [1] Tokk model turbine test report, 2007.
- [2] Hermod Brekke. *Pumper & turbiner*. Waterpower Laboratory, NTNU, 2003.
- [3] Hermod Brekke. *Konstruksjon av pumper og turbiner*. Waterpower Laboratory, NTNU, 2008.
- [4] Ole Gunnar Dahlhaug. Personal conversation, Spring 2014.
- [5] Mette Eltvik, Pål Henrik Finstad, Grunde Olimstad, Eve Walseth, and Zhao Wei. High pressure hydraulic machinery. Technical report, Waterpower Laboratory, NTNU, Autumn 2009.
- [6] Anders Flaten. Conversation, Spring 2014.
- [7] A. Gebhardt. *Understanding Additive Manufacturing: Rapid Prototyping, Rapid Tooling, Rapid Manufacturing*. Carl Hanser Verlag, 2011.
- [8] Kristine Gjørseter. Hydraulic design of francis turbine exposed to sediment erosion. Master's thesis, NTNU, Spring 2011.
- [9] Kerb Konus GmbH. Kerb konus's webpage. <http://www.kerbkonus.de/>, 2014.
- [10] Peter Joachim Gogstad. Hydraulic design of francis turbine exposed to sediment erosion. Master's thesis, NTNU, Fall 2011.
- [11] Arrk Europe Ltd. Arrk europe's webpage. <http://www.arrkeurope.com/>, 2014.
- [12] Torbjørn K. Nielsen. TEP4195 Turbomachinery, Lecture, Spring 2013.
- [13] Inc. PTC. Ptc's webpage. <http://www.ptc.com/product/creo//>, 2014.

Appendix A

Appendix A

A.1 Guide vane calculations

In this appendix some simple calculations on the guide vanes and runner vanes will be shown.

Data from Tokke model turbine test		
Head	$H = 30$	[m]
Rotational speed	$n = 540$	[RPM]
Number of guide vanes	$Z_0 = 28$	[$-$]
Inlet diameter	$D_1 = 3.17$	[m]

Table A.1: Data from Tokke model test used in calculations

A.1.1 Hydraulic force on guide vane in closed position

Some of the values used in the calculations are taken from the 3D model in Creo; $B_0 = 0.05938[m]$, $a_0 = 0.01015[m]$, $l = 0.07921[m]$, $D_0 = 0.70595[m]$, $d = 0.014/0.020$, .
The total force on each vane:

$$F_0 = \rho g H B_0 l = \frac{\pi \rho g H B_0 D_0}{z_0} = \frac{\pi \cdot 1000 \cdot 9.81 \cdot 30 \cdot 0.05938 \cdot 0.70596}{28} = 1384.2 [N] \quad (A.1)$$

The torque, T_0 , on one guide vane tap is then:

$$T_0 = F_0 \cdot a_0 = 1384 \cdot 0.01015 = 14.05 [Nm] \quad (A.2)$$

The polar moment of inertia, I_P for the guide vane shaft:

$$I_P = \frac{\pi \cdot d^4}{32} = \frac{\pi \cdot 0.014^4}{32} = 3.77 \cdot 10^{-9} [m^4] \quad (A.3)$$

The maximum shear stress, τ_{max} , due to torque is then found:

$$\tau_{max} = -\tau_{max} = \frac{T_0}{I_P} \cdot r = \frac{14.05 \cdot 0.007}{3.77 \cdot 10^{-9}} = 26.08 [MPa] \quad (A.4)$$

Bending moment:

$$M = \frac{\pi \rho g H_0 B_0^2 D_0}{8 z_0} = \frac{\pi \cdot 1000 \cdot 9.81 \cdot 30 \cdot 0.05938^2 \cdot 0.70596}{8 \cdot 28} = 10.3 [Nm] \quad (A.5)$$

Moment of inertia:

$$I_P = \frac{\pi \cdot d^4}{64} = \frac{\pi \cdot 0.014^4}{64} = 1.89 \cdot 10^{-9} [m^4] \quad (A.6)$$

Bending stress:

$$\sigma_b = \frac{M \cdot r}{I_X} = \frac{10.3 \cdot 0.007}{1.89 \cdot 10^{-9}} = 38.15 [MPa] \quad (A.7)$$

The lages pricipal stress is then calculated by:

$$\sigma_{max} = \frac{\sigma_b}{2} \pm \sqrt{\frac{\sigma_b^2}{4} + \tau^2} = \frac{38.15}{2} + \sqrt{\frac{38.15^2}{4} + 26.08^2} = 51.4 [MPa] \quad (A.8)$$

Appendix **B**

Appendix B

B.1 Price offer from Protolab AS

In this appendix there is a review of the different price offer received from Protolab AS. T

B.1.1 Price on

Protolab AS

Prof. Brochs gt 8A
NO-7030 TRONDHEIM
Norge
Telefon 40413726 Bank 50810753959
E-post: firmapost@protolab.no
www.protolab.no
Org.nr.NO 989 645 501 MVA

Tilbud 467

Side 1
Kundenr. 32744
Prosjekt PL-74114 NTNU Stud
Avdeling
Leveringsform Postpakke
Lev. betingelser Mottaker betaler frakt
Valuta NOK
Tilbudsdato 30.01.2014
Bet. betingelser Netto 20 dager
Gyldig t.o.m. 30.03.2014

Rundhaug, Kristoffer, NTNU Stud

Norge

Vår ref. Anders Flaten
Deres ref. Kristoffer Rundhaug
Referanse Forespørsel skovler SERIE

<i>Produktnr.</i>		<i>Antall</i>	<i>Antall lev.</i>	<i>Enhetspris</i>	<i>Mva.</i>	<i>Sum</i>
100003	SLS-modell i SLA-HST (PA) m/sealing <helskovl>	15,00	15,00	2 835,00	25,00%	42 525,00
100003	SLS-modell i SLA-HST (PA) m/sealing <halvskovl>	15,00	15,00	1 430,00	25,00%	21 450,00
Mva. %	Mva-grunnlag					Mva.
25,00 %	63 975,00					15 993,75

Prototyper i SLS-HST (High Strength PA)
Leveringstid: ca 14 dager.

<i>Netto</i>	<i>Mva.</i>	<i>Sum inkl. mva.</i>
63 975,00	15 993,75	79 969,00

Figure B.1: Price offer for a full set of runner vanes to the Tokke model runner

Protolab AS

Prof. Brochs gt 8A
 NO-7030 TRONDHEIM
 Norge
 Telefon 40413726 Bank 50810753959

E-post: firmapost@protolab.no
 www.protolab.no
 Org.nr.NO 989 645 501 MVA

Rundhaug, Kristoffer,NTNU Stud

Norge

Vår ref. Anders Flaten
 Deres ref. Kristoffer Rundhaug
 Referanse Forespørsel skovler PILOT

Tilbud 466

Side 1
 Kundenr. 32744
 Prosjekt PL-74114 NTNU Stud
 Avdeling
 Leveringsform Postpakke
 Lev.betingelser Mottaker betaler frakt
 Valuta NOK
 Tilbudsdato 30.01.2014
 Bet. betingelser Netto 20 dager
 Gyldig t.o.m. 30.03.2014

Produktnr.		Antall	Antall lev.	Enhetspris	Mva.	Sum
100003	SLS-modell i SLA-HST (PA) m/sealing <helskovl>	2,00	2,00	4 405,00	25,00%	8 810,00
100003	SLS-modell i SLA-HST (PA) m/sealing <chalvskovl>	2,00	2,00	2 155,00	25,00%	4 310,00
Mva. %	Mva-grunnlag					Mva.
25,00 %	13 120,00					3 280,00

Prototyper i SLS-HST (High Strength PA)
 Leveringstid: 6-8 dager

Netto	Mva.	Sum inkl. mva.
13 120,00	3 280,00	16 400,00

Figure B.2: Price offer for a couple of test vanes to the Tokke model runner

Protolab AS

Prof. Brochs gt 8A
NO-7030 TRONDHEIM
Norge
Telefon 40413728 Bank 50810753969

E-post: firmapost@protolab.no
www.protolab.no
Org.nr.NO 989 645 501 MVA

NTNU Institutt for Energi og Prosessteknikk
Alfred Getzs vei 4
NO-7491 TRONDHEIM
Norge

Tilbud 480

Side 1
Kundenr. 32744
Prosjekt PL-74114 NTNU Stud
Avdeling
Leveringsform Postpakke
Lev.betingelser Fritt levert
Valuta NOK
Tilbudsdato 27.03.2014
Bet. betingelser Netto 20 dager
Gyldig t.o.m. 27.05.2014

Vår ref. Anders Flaten
Deres ref. Kristoffer Rundhaug
Referanse Forespørsel skovler HST

Produktnr.		Antall	Antall lev.	Enhetspris	Mva.	Sum
100003	SLS-modell i SLA-HST m/sealing	1,00	1,00	1 985,00	25,00%	1 985,00
	<test_1>					
100003	SLS-modell i SLA-HST m/sealing	1,00	1,00	1 105,00	25,00%	1 105,00
	<test_2>					
Mva. %	Mva-grunnlag			Mva.		
25,00 %	3 090,00			772,50		

Prototyper i SLS-HST (High Strength PA)
Leveringstid: 6-8 dager

Netto	Mva.	Sum inkl. mva.
3 090,00	772,50	3 863,00

Figure B.3: Price offer for test piece in SLS material DuraForm HST

Protolab AS

Prof. Brochs gt 8A
 NO-7030 TRONDHEIM
 Norge
 Telefon 40413726 Bank 50810753959

E-post: firmapost@protolab.no
 www.protolab.no
 Org.nr.NO 989 645 501 MVA

NTNU Institutt for Energi og Prosessteknikk
 Alfred Getzs vei 4
 NO-7491 TRONDHEIM
 Norge

Tilbud 481

Side 1
 Kundenr. 32744
 Prosjekt PL-74114 NTNU Stud
 Avdeling
 Leveringsform Postpakke
 Lev.betingelser Fritt levert
 Valuta NOK
 Tilbudsdato 27.03.2014
 Bet. betingelser Netto 20 dager
 Gyldig t.o.m. 27.05.2014

Vår ref. Anders Flaten
 Deres ref. Kristoffer Rundhaug
 Referanse Forespørsel skovler PA

Produktnr.		Antall	Antall lev.	Enhetspris	Mva.	Sum
100003	SLS-modell i SLA-PA m/sealing <test_1>	1,00	1,00	1 570,00	25,00%	1 570,00
100003	SLS-modell i SLA-PA m/sealing <test_2>	1,00	1,00	905,00	25,00%	905,00
Mva. %	Mva-grunnlag			Mva.		
25,00 %	2 475,00			618,75		

Prototyper i SLS-PA
 Leveringstid: 6-8 dager

Netto	Mva.	Sum inkl. mva.
2 475,00	618,75	3 094,00

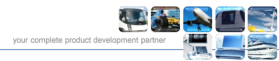
Figure B.4: Price offer for test pice in SLS material DuraForm PA

Appendix C

Appendix C

C.1 Material properties

Protolab AS use ARRK Europe LTD as their manufacturer of prototypes. Here is a overview of the material properties for the material from different



SELECTIVE LASER SINTERING (SLS) MATERIAL RANGE. MATERIAL PROPERTIES (for comparative purposes only).

General Properties	Method	Value		Value	
		DuraForm PA	Polyamide Glass-Filled	DuraForm HST	Ex (White)
Specific Gravity	ASTM D792	1.00 g/cm ³	1.49 g/cm ³	1.20g/cm ³	1.01 g/cm ³
Moisture Absorption – 24 hours	ASTM D570	0.07%	0.22%	N/A	0.46%
Moisture Saturation	ASTM D570	N/A	N/A	N/A	1.16%
Tensile Strength, Yield	ASTM D638	N/A	27 MPa	N/A	37 MPa (5366 psi)
Tensile Strength, Ultimate	ASTM D638	43 MPa	26 MPa	48-51 MPa	48 MPa (6961 psi)
Tensile Modulus	ASTM D638	1986 MPa	4068 MPa	5475 -5725 MPa	1517 MPa (220 ksi)
Elongation at Yield	ASTM D638	N/A	1.4%	N/A	5%
Elongation at Break	ASTM D638	14%	1.4%	4.5%	47%
Flexural Strength, Yield	ASTM D790	N/A	N/A	N/A	42 MPa (6091 psi)
Flexural Strength, Ultimate	ASTM D790	48 MPa	37 MPa	83-89 MPa	46 MPa (6672 psi)
Flexural Modulus	ASTM D790	1387 MPa	3106 MPA	4400-4550 MPa	1310 MPa (190 ksi)
Hardness , Shore D	ASTM D2240	73	77	75	74
Hardness, Rockwell L	ASTM D785	N/A	N/A	N/A	69
Hardness, Rockwell M	ASTM D785	N/A	N/A	N/A	34
Impact Strength (notched Izod, 23°C)	ASTM D256	32 J/m	41 J/m	37.4 J/m	74 J/m (1.4 ft-lb/in)
Impact Strength (unnotched Izod, 23°C)	ASTM D256	336 J/m	123 J/m	310 J/m	1486 J/m (>27.8 ft-lb/in)
Gardner Impact	ASTM D6420	2.7 J	4.5 J	5 J	11.8 J (8.7 ft-lb)
Heat Deflection Temperature	ASTM D648				
@ 0.45 MPa		180 °C	179 °C	184°C	188 °C (370 °F)
@ 1.82 MPa		95 °C	134 °C	179°C	48 °C (118 °F)
Coefficient of Thermal Expansion	ASTM E831				
@ 0-50 °C		82.3 µm/m-°C	82.6 µm/m-°C	139.3 µm/m-°C	120 µm/m-°C (66.7 µin/in-°F)
@ 85-145 °C		124.6 µm/m-°C	179.2 µm/m-°C	148.4 µm/m-°C	342 µm/m-°C (190 µin/in-°F)
Specific Heat Capacity	ASTM E1269	1.84 J/g-°C	1.09 J/g-°C	1.503 J/g-°C	1.75 J/g-°C (0.418 BTU/lb-°F)
Thermal Conductivity	ASTM E1225	0.70 W/m-K	0.47 W/m-K		0.51 W/m-K (3.5 BTU-in/hr-ft ² -°F)
Flammability	UL94	HB	HB	HB	HB
Volume Resistivity	ASTM D297	5.9 x 10 ¹⁰ ohm-cm	3.2 x 10 ¹⁰ ohm-cm	6.7 x 10 ¹⁵ ohm-cm	1.3 x 10 ¹⁰ ohm-cm
Surface Resistivity	ASTM D297	7.0 x 10 ¹⁰ ohm	3.2 x 10 ¹⁰ ohm	5.2 x 10 ¹⁵ ohm	4.9 x 10 ¹⁰ ohm
Dissipation Factor, 1 KHz	ASTM D150	0.044	0.177	0.028	0.050
Dielectric Constant, 1 KHz	ASTM D150	2.73	6.27	3.14	4.5
Dielectric Strength	ASTM D149	17.3 kV/mm	8.7 kV/mm	18.5 kV/mm	18.5 kV/mm (470 kV/in)

www.arrkeurope.com

Figure C.1: Material range at ARRK for SLS printing



Rapid CNC Machining

ARRK are able to offer customers a wide range of CNC machining options from our new rapid CNC centre at Gloucester, plus larger volumes manufactured out of ARRK facilities in the Far East.

Rapid CNC machining - available here in the UK as well as in the Far East

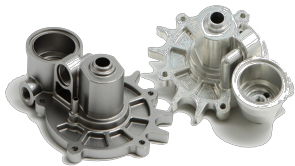
If you are looking for a rapid turnaround of machined parts within a matter of days our new **UK Rapid CNC Cell in Gloucester** could be the perfect solution for you.

With a range of Mazak and DMG machines, offering 5 and 3 axis capability, our new centre has been set up to satisfy our customers' increasing demand for speedy delivery. Whether you need just a single component or a number of machined parts we can help.

CNC machined components - through to Block Modelling, Texturing and Finishing

Alternatively, where customers are looking for more complex machining or post machining options, our facilities in the Far East provide even **greater CNC capacity and services**. The ARRK team in the Far East has built up an impressive reputation for taking complex, intricate projects and making them a reality.

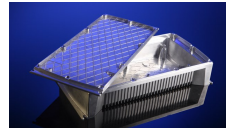
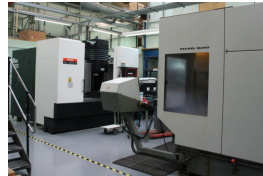
prototyping



ARRK are able to cut from a wide range of plastics and metals, from standard materials to the more unusual.

Out standard range includes:

Material	Trade Name
ABS	Tecaran
Acetal	Tecaran
Acrylic	Tecaform AH
Cast Nylon	Tecast
Delrin	Tecanyl
Nylon 6	Tecamid 6
Nylon 66	Tecamind 66
Nylon 12	Tecamid 12
PEEK	Tecapeek
Petg	Petg
Polycarbonate	Tecanat
Polyester	Tecapet
Polyethersulphone	Tecason E
Polyphenylenesulphone	Tecason P
Polyethylene	Tecafine PE
Uhmw PE	Tecafine PE10
Polyimide	Tecasint
Polypropylene	Tecafine PP
Polysulphone	Tecason S
PPS	Tecastron
PTFE	Tecasflon PTFE
PVC	Tecavinyl
PVDF	Tecaflon PVDF
Tufnol®	Tufnol®
Ultem®	Tecapei
AL/AL Plate 6082	
AL/AL Plate 5083	
AL/AL Plate 7075	
Brass Plate	
Brass Bar	
Copper Plate	
Copper Bar	
Zinc Plate	
Mild Steel Plate	
Stainless Steel Plate 304/316 Sheared	
Stainless Steel Plate 304/316 Plasma	
Stainless Steel Plate 304/316 Sawn	





Why use ARRK's CNC Service

- Speed of delivery
- Huge capacity
- We can start your project quickly
- Great part quality
- Wide range of material options
- Vast experience
- Models that are simply stunning
- Highly competitive service and rates

For more information, please contact:

Gloucester Technical Centre. Olympus Park,
 Quedgeley, Gloucester. GL2 4NF, UK.

Tel: +44(0)1452 727700

Fax: +44 (0)1452 727755

E-mail: projects@arrkeurope.com

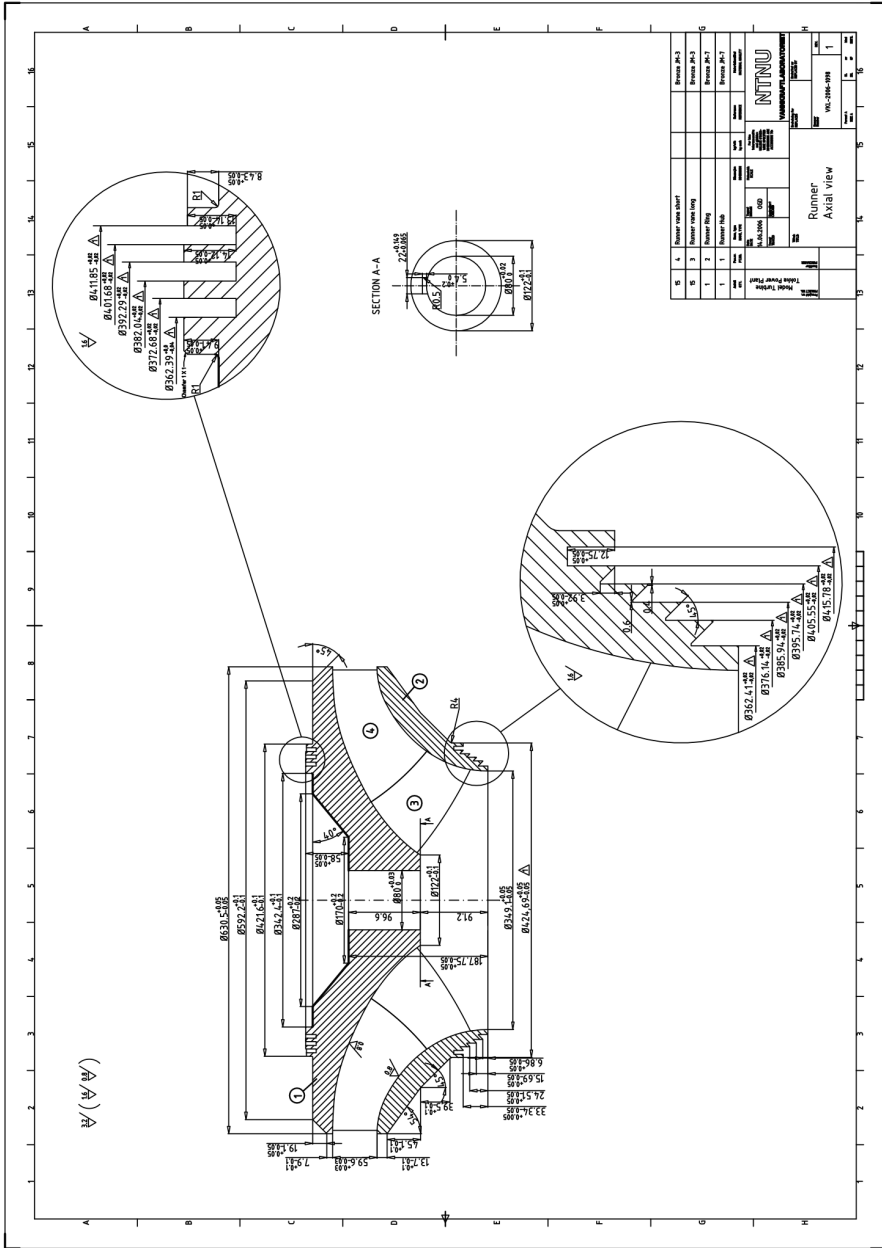


Appendix **D**

Appendix D



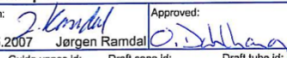
D.1 Drawings and documents from Tokke model turbine

In this appendix the drawings of Tokke model runner, guide vanes, stay vanes and stay ring used to make the new designs fit the Francis model rig at the Waterpower laboratory at NTNU.



7-100

Figure D.1: Axial view of the Tokke model runner

		Waterpower laboratory NTNU				End: 16.4321		
		Project id: TOKKE				Data files:		
		Document: Test record Guide vane torque measurement VKL runner				VKL3-020507-2.txt		
		Proj. no. -Test series:	Date/Sign:	Approved:				
		340298.00- 3	02.05.2007					
Model id: VKL-1	Main section id: TOKKE 1	Runner id: VKL-2006-1098	Spiral case id: VKL-2006-1018	Stay vanes id: VKL-2006-1036	Guide vanes id: VKL-2006-1029	Draft cone id: VKL-2006-1010	Draft tube id: VKL-2006-1000	Comments:

Guide vane torque for VKL-runner at $H_M=30$ and $n_{gM}=540$

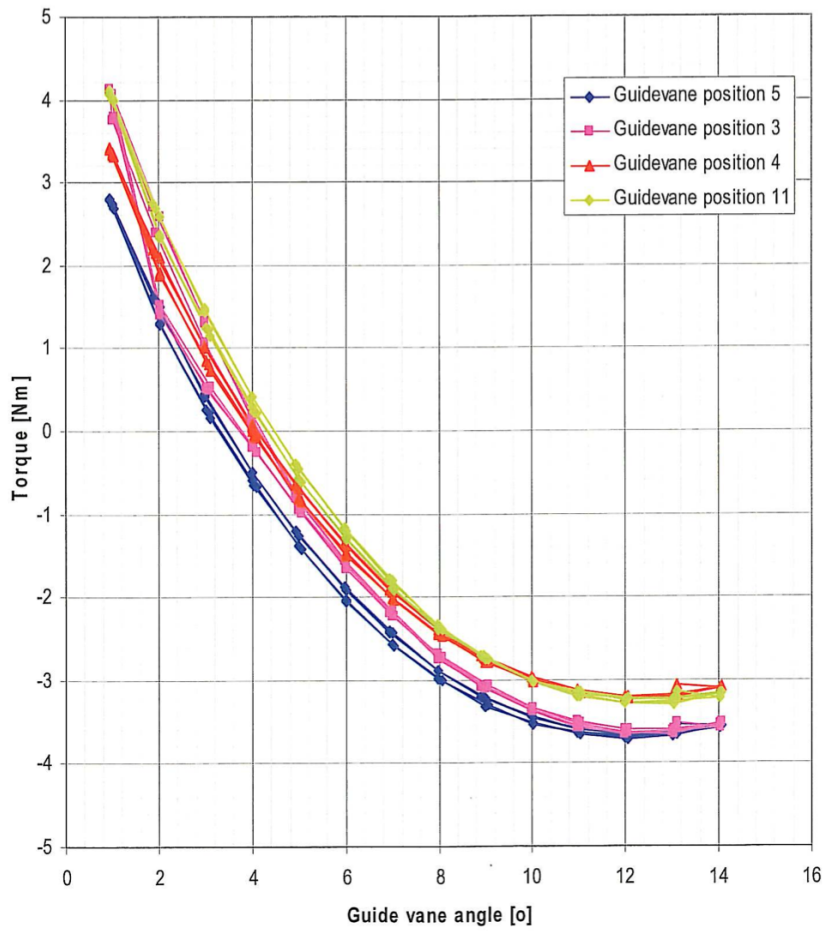
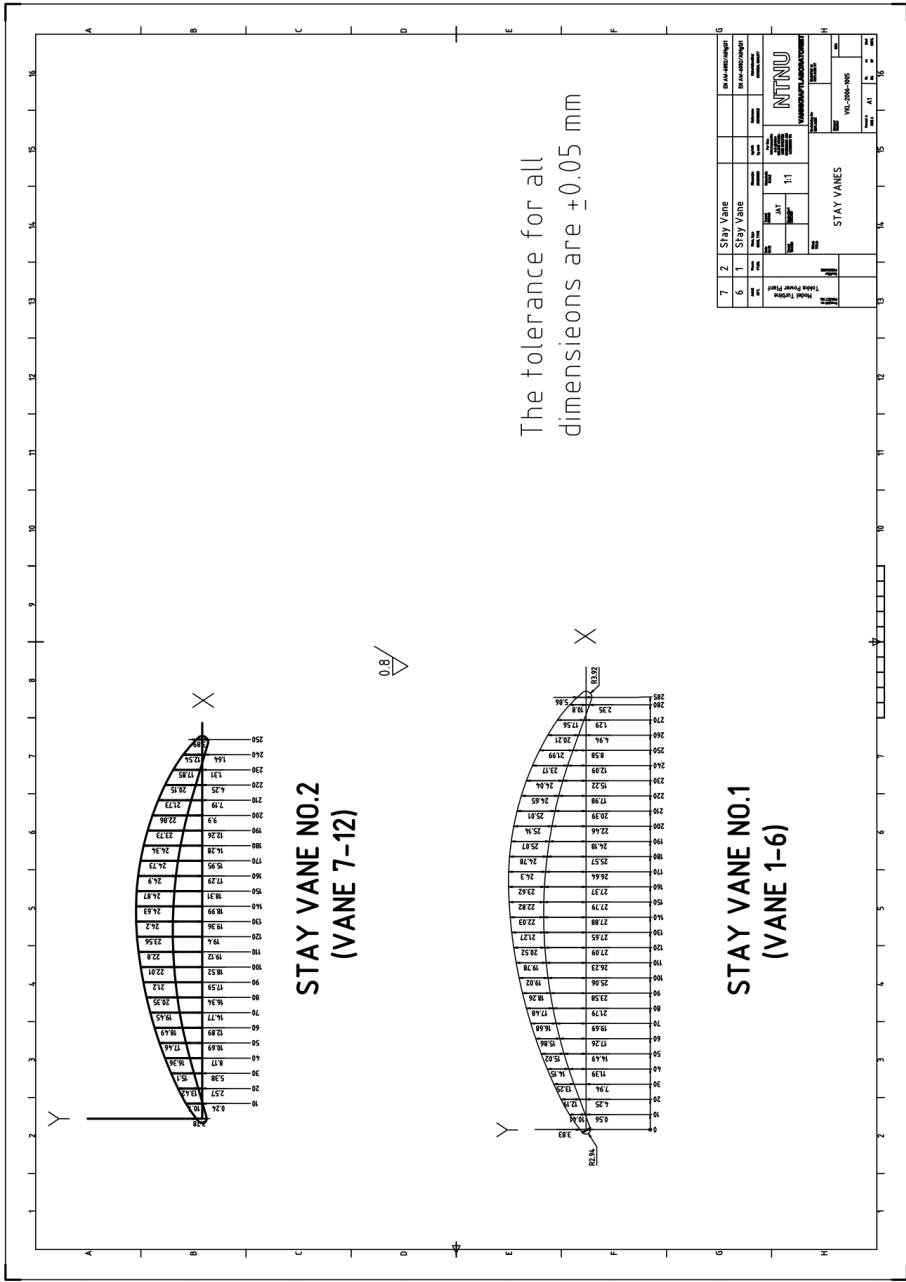
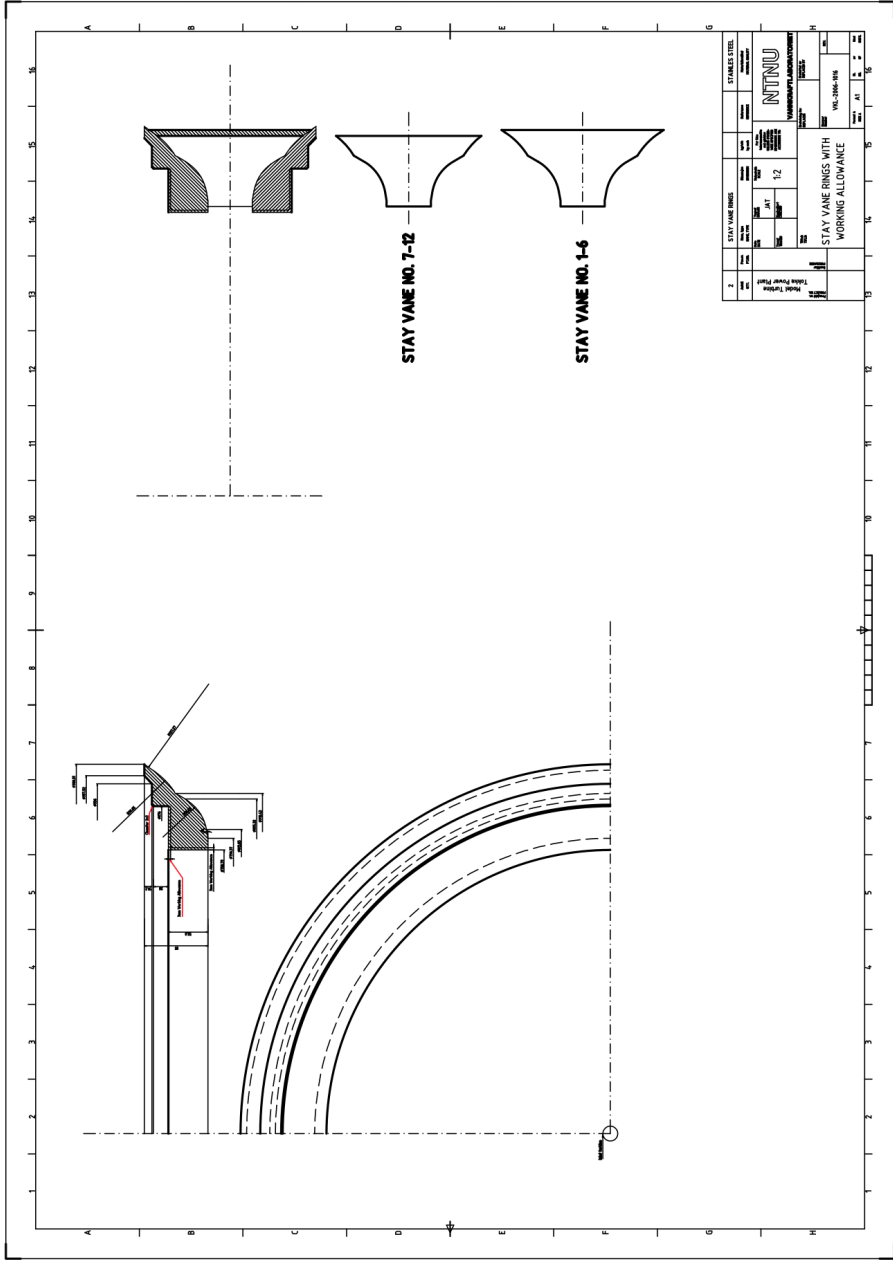


Figure D.3: Guide vane torque for VKL-runner [1]



7-8

Figure D.4: Drawing of the stay vane shapes



7-19

Figure D.5: Drawing of the stay ring

Appendix **E**

Appendix E

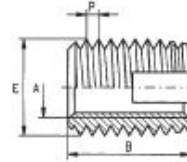
E.1 Product information sheets for the fixing parts

In this appendix the product information sheets for the parts used to fasten the runner vanes to the hub and shroud are shown.

Application

The threaded insert with cutting slot is a self-tapping fastener for the creation of wear-free, vibration resistant screw joints with high loading capacity in materials with low shearing strength.

It is suitable for installation in the following materials:
 - Plastic, laminates
 - Hardwood, but also
 - Light alloys
 - Cast iron, brass, bronze
 NF metals
 For technical information see Publication 20



Dimensions in mm

Article no.	Internal thread A	External thread		Length B	Guideline values for receiving hole dia. L	Minimum drill hole depth in case of blind holes T
		E	P			
302 000 020 ...	M 2	4,5	0,5	6	4,1 to 4,2	8
302 000 025 ...	M 2,5	4,5	0,5	6	4,1 to 4,2	8
302 000 030 ...	M 3	5	0,5	6	4,6 to 4,7	8
302 000 035 ...	M 3,5	6	0,75	8	5,5 to 5,6	10
302 000 040 ...	M 4	6,5	0,75	8	6,0 to 6,1	10
302 000 050 ...	M 5	8	1	10	7,3 to 7,5	13
302 000 061 ...	M 6 (2)	9	1	12	8,3 to 8,5	15
302 000 060 ...	M 6	10	1,5	14	8,9 to 9,2	17
302 000 080 ...	M 8	12	1,5	15	10,9 to 11,2	18
302 000 100 ...	M 10	14	1,5	18	12,9 to 13,2	22
302 000 120 ...	M 12	16	1,5	22	14,9 to 15,2	26
302 000 140 ...	M 14	18	1,5	24	16,9 to 17,2	28
302 000 160 ...	M 16	20	1,5	22	18,9 to 19,2	27
302 000 180 ...	M 18	22	1,5	24	20,9 to 21,2	29
302 000 200 ...	M 20	26	1,5	27	24,9 to 25,2	32
302 000 220 ...	M 22	26	1,5	30	24,9 to 25,2	36
302 000 240 ...	M 24	30	1,5	30	28,9 to 29,2	36
302 000 270 ...	M 27	34	1,5	30	32,9 to 33,2	36
302 000 300 ...	M 30	36	1,5	40	34,9 to 35,2	46

Example for finding the article number

Self-tapping threaded insert Ensat-S to Works Standard series 302 with internal thread A = M5 made of case-hardened, zinc plated and yellow chromated, steel: Ensat-S 302 000 050.160

Materials

Unhardened steel	Article no. 100
Case-hardened steel, zinc plated, blue passivated	Article no. 110
Case-hardened steel, zinc/nickel plated, transparent passivated	Article no. 143
Case-hardened steel, zinc plated, yellow chromated	Article no. 160
Stainless steel 1.4105	Article no. 400
Stainless steel 1.4305	Article no. 500
Brass	Article no. 800
Other materials, designs and finishes on request.	

Tolerances

ISO 2768-m

Thread

Internal thread A: as per ISO 6H
 External thread E: metric, tolerances in accordance with Works Standard
 Internal thread UNC, UNF; Whitworth, see page 9

Remark:

M2/M2,5 only for materials with minimal strength, as the shearing resistance of the studs in the installation tools may be insufficient.

Figure E.1: Product info about Kerb Konus threaded inserts Ensat S


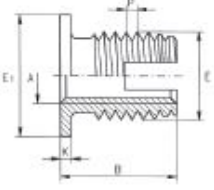
	Threaded insert self-tapping		Ensat®-SK Works Standard 302 1				
Application Threaded insert Ensat-SK 302 1 with cutting slot and head is a self-tapping fastener for the creation of wear-free, vibration-resistant screw joints with high loading capacity in materials with low shearing strength.	It is suitable for installation in the following materials: - Light alloys - Cast iron, brass, bronze, NF metals - Plastics, laminates - Hardwoods.		The head serves as a support for electrical contacts, for simultaneous fixture of several parts; when stress is applied against the head, the pull-through force is significantly increased. 				
Dimensions in mm							
Article no.	Internal thread A	External thread E P		Head diameter E1	Head height K	Length B	Minimum borehole depth for blind holes T
302 100 040 ...	M 4	6,5	0,75	9	1	9	10
302 100 050 ...	M 5	8	1	11	1	11	12
302 100 060 ...	M 6	10	1,5	13	1,5	15,5	16
302 100 080 ...	M 8	12	1,5	15	1,5	16,5	17
302 100 100 ...	M 10	14	1,5	17	1,5	19,5	20
Example for finding the article number	Self-tapping threaded insert Ensat-SK with head to Works Standard series 302 1 with internal thread A = M5 made of case-hardened, zinc plated and yellow chromated steel: Ensat-SK 302 100 050.160						
Materials	Unhardened steel Case-hardened steel, zinc plated, blue passivated Case-hardened steel, zinc/nickel plated, transparent passivated Case-hardened steel, zinc plated, yellow chromated Brass Other materials, designs and finishes on request.		Article no. (fourth group of digits) 100 Article no. (fourth group of digits) 110 Article no. (fourth group of digits) 143 Article no. (fourth group of digits) 160 Article no. (fourth group of digits) 800				
Tolerances	ISO 2768-m						
Thread	Internal thread A: as per ISO 6H External thread E: metric, tolerances in accordance with Works Standard Internal thread UNC, UNF, Whitworth or fine thread on request						
For details of bore diameter guideline values, see the table on page 6							

Figure E.2: Product info about Kerb Konus threaded inserts Ensat SK

Application

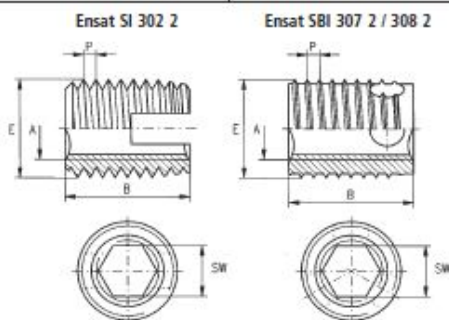
This threaded insert with hexagonal socket is a self-tapping fastener for the creation of low-wear, vibration resistant screw joints with high load capacity in materials with low shearing strength.

The Ensat is inserted via the hexagonal socket, permitting the achievement of short installation times.

Other benefits: More simple driving tools and machines which require only clockwise rotation.

When using in plastics, the Ensat can be extracted without problems before the recycling process, resulting in lower costs. It is suitable for installation in the following materials:

- Duroplastics, thermoplastics (with the exception of rubber-soft thermoplastics < 100 Shore A)
- but also for
- Aluminium and aluminium alloys
- Magnesium alloys



Dimensions in mm

Article no.	Internal thread	External thread (Special thread)		Length	Hexagonal socket	Minimum drill hole depth in case of blind holes	Guideline values for receiving hole dia.
	A	E	P		B		
302 200 040 ...	M 4	6,5	0,75	8	3,2	10	6,0 to 6,1
307 200 040 ...			6	6	3,2	8	
308 200 040 ...			0,8	8	3,2	10	
302 200 050 ...	M 5	8	1	10	4,1	13	7,4 to 7,6
307 200 050 ...			7	7	4,1	9	
308 200 050 ...			1	10	4,1	13	
302 200 060 ...	M 6	10	1,5	14	4,9	17	9,3 to 9,5
307 200 060 ...			1,25	8	4,9	11	
308 200 060 ...			1,25	12	4,9	15	
302 200 080 ...	M 8	12	1,5	15	6,6	18	11,1 to 11,3
307 200 080 ...			1,5	9	6,6	12	
308 200 080 ...			1,5	14	6,6	17	
302 200 100 ...	M 10	14	1,5	18	8,3	22	13,1 to 13,3
307 200 100 ...			1,5	10	8,3	16	
308 200 100 ...			1,5	18	8,3	22	
302 200 120 ...	M 12	16	1,5	22	10,1	27	15,0 to 15,2
307 200 120 ...			1,75	12	10,1	15	
308 200 120 ...			1,75	22	10,1	26	

Example for finding the article number

Self-tapping threaded insert Ensat-SBI to Works Standard series 308 2 with internal thread A = M 5 made of case-hardened, zinc plated and yellow chromated, steel: Ensat-SBI 308 200 050.160

Materials

Case-hardened steel, zinc plated, blue passivated
Case-hardened steel, zinc plated, yellow chromated
Brass
Other materials on request.

Article no. 110
Article no. 143
Article no. 160
Article no. 800

Tolerance

ISO 2768-m

Thread

Internal thread A: as per ISO 6H
External thread E: Special thread with flattened thread root, tolerance in accordance with Works Standard

Figure E.3: Product info about Kerb Konus threaded inserts Ensat SI/SBI

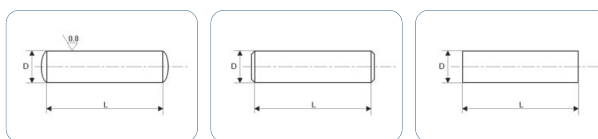
GOUPILLES CYLINDRIQUES
DOWEL PINS

GOUPILLES CYLINDRIQUES
ISO2338 - NFE27484
DOWEL PINS - ISO2338 - NFE27484



- ☒ Désignation : Goupilles cylindriques ISO2338 [forme] D x L
Description: Dowel pins ISO2338 DxL
- ☒ Forme A : D = tolérance m6 / Forme B : D = tolérance h8 /
Forme C : D = tolérance h11
A shape: D = tolerance m6 / B shape: D = tolerance h8 / C shape: D = tolerance h11

ATTENTION : Bien choisir la forme des extrémités et la tolérance
Please note: choose the right shape and tolerance for your needs



Matière = 95MnPb28K et inox
Material: 95MnPb28K and stainless steel

D	L																										
1	3	4	6	8	10	12	14	16	18	20																	
1,5	3	4	6	8	10	12	14	16	18	20	22	24	26	28	30	32											
2		4	6	8	10	12	14	16	18	20	22	24	26	28	30	32	36	40									
2,5		4	6	8	10	12	14	16	18	20	22	24	26	28	30	32	36	40									
3		4	6	8	10	12	14	16	18	20	22	24	26	28	30	32	36	40	45	50							
4			6	8	10	12	14	16	18	20	22	24	26	28	30	32	36	40	45	50	55	60					
5			6	8	10	12	14	16	18	20	22	24	26	28	30	32	36	40	45	50	55	60					
6			6	8	10	12	14	16	18	20	22	24	26	28	30	32	36	40	45	50	55	60					
8				10	12	14	16	18	20	22	24	26	28	30	32	36	40	45	50	55	60	70	80				
10					12	14	16	18	20	22	24	26	28	30	32	36	40	45	50	55	60	70	80	90	100		
12						12	14	16	18	20	22	24	26	28	30	32	36	40	45	50	55	60	70	80	90	100	120

Boîtes assortiments goupilles voir p.25
Boxed sets of pins, see p.25

- SUR DEMANDE** • Dimensions et tolérances spéciales
ON REQUEST • Other tolerances and dimensions
- Matières spéciales notamment en inox
Special materials, particularly stainless steel

Figure E.4: Product information about the DIN 7 pins